Experiments with sea spray icing: Investigation of icing rates

Sujay Deshpande*, Ane Sæterdal, Per-Arne Sundsbø

Dept. of Building, Energy and Material Technology, UiT, The Arctic University of Norway.
*Corresponding author: Sujay Deshpande.
Address: C/o UiT, Campus Narvik, Lodve Langesgate 2, 8514, Narvik, Norway.
email: sujay.r.deshpande@uit.no

Abstract

Sea spray icing on ships and marine structures depends on a complex correlation between metocean parameters and vessel characteristics. Sea spray icing rates have mostly been investigated and given as a function of general metocean parameters. The existing models suffer from lack of experimental data. More experimental data is required for better prediction models and understanding of the icing process. This paper presents results from a comprehensive cold laboratory study of the dependence and trends of sea spray icing rates related to 8 parameters. Experiments were performed simulating sea spray from a nozzle towards a vertical surface in freezing environment. This study presents 20 unique tests structured into 8 experiments, each of which focusses on change in icing rates due to one independent variable. Results showed that the sea spray rates dependence of the investigated parameters comply with existing knowledge, however preliminary analysis points out various unintentional covariates for most experiments which calls for further investigations. This is the greatest number of variables tested in one set of experiments to date and serve as valuable sea spray icing data experimental data – a limitation for the evaluation of previous models that pointed out to the lack of enough icing measurements in this field of research.

Keywords: Sea spray icing, icing on ships and offshore structures, experimental icing data, icing rates.

1. Introduction

Arctic and Sub-Arctic regions have seen a growth in marine and offshore operations in terms of fishing, aquaculture installations, oil and gas exploration, and more recently, tourism. Marine operations in cold climate have numerous challenges out of which, sea spray icing has been pointed out to be a major challenge. Sea spray icing, possibly in combination with snow [1], has been attributed to 80-90% of all offshore icing incidents [2]. Icing predictions are essential for safe marine operations. Winterization of vessels and offshore structures includes anti-icing and de-icing procedures that require estimation of expected icing already at the design stage [3].

Previously, researchers have presented models for the prediction of sea spray icing [4]–[9]. A recent review article suggests need for improvement of these models and points out to the lack of enough full-scale and laboratory experimental data studying sea spray icing [3].

Full scale measurements for sea spray icing were carried out by some researchers [10], [11]. However, large variations were expected due to limitations in measurement techniques and the measurements

were not detailed enough for validation of computational results [3]. Laboratory experiments were conducted by Stallabrass & Hearty, 1967 for studying sea spray icing in cylinders [12]. Variation of atmospheric temperature was the only variable in this experiment. In reality, sea spray icing is a complex process including numerous uncertain variables [3].

Deghani-Sanij et.al., 2019 presented an experimental study for sea spray icing that analyzed mass and thickness due to sea spray icing with 12 unique sets of measurement. This was a major step forward into experimentation with multiple variables for sea spray icing. The experiment consisted of two variations each of atmospheric temperature and salinity, 3 variations of wind speeds, and 2 variations of a combination of spray duration and spray period. This experiment did not include sea temperature as a variable which was measured at 20.9°C in the water tank outside the freezing room, and about 17°C measured in pipe just before the nozzle inside the freezing room. The temperature in the freezing rooms during the experiments varied by 4°C during the tests. [13]

The current study presents results from a set of 20 unique tests in which 8 different variables identified to affect sea spray icing were tested under controlled conditions in the cold climate laboratory at UiT, The Arctic University of Norway, Campus Narvik. The study is divided into 9 different experiments (8 variables + 1 repeatability) with either 3 or 4 tests included in each experiment. In each experiment, one variable is varied for individual tests while keeping the others constant to study the effects of individual variables on icing rates. The results of the tests are presented in the form of icing rates on a vertical plate in terms of weight and thickness. In a first, the time dependency of icing rates in the initial stages of an icing event is presented. Some parameters are difficult to be kept constant even under laboratory conditions and thus the difference between ideal and practical conditions are presented for every test. The variation due to different measurement methods is part of the study. The results presented in this article illustrates how icing rates could vary the selected variables and methods of measurement. However, owing to the relatively large scope of the experiments, detailed level of measurements, and the fact that many of the variables cannot be kept constant even under controlled laboratory conditions, it is not straightforward to investigate the connection to existing sea spray models based on metocean parameters. However, the provided experimental data of the icing process show important trends that would be useful for further analysis. The complete lab setup and lessons learned during the experimental work and data collection are shared to assist improvements during any similar experiments in the future. Data analysis with the help of machine learning, interpretation of the results in terms of metocean conditions and ship characteristics, and comparison of results with existing models is suggested as a progression for this study.

2. Selection of variables

Sea spray icing is a complex process involving many variables, some of which are difficult to measure to full extent or be controlled in an experimental setup. Different researchers also had very different approaches to prediction models and selection of governing variables in the icing process.

The simplest of the models is an empirical model presented by Overland 1986 based on statistical analysis of metocean data, that predicts the icing thickness rate (cm/hr) from wind speed (U_{10}), air and sea temperatures, and the freezing point of water, that is a function of salinity [8], [10]. Stallabrass 1980

presented a stationary theoretical model for the prediction of icing thickness rate (mm/hr) using wave height, relative wind speed, temperature of icing surface, air temperature, spray droplet temperature at impingement, sea temperature, thermal conductivity of air, Nusselt number for wind flow, density of water, specific heat of water, droplet diameter, latent heat of vaporization, barometric pressure, specific heat of dry air, vapour pressure at air temperature and at droplet temperature at impingement [9]. Kulyakhtin 2014, used a hybrid theoretical and numerical model for predicting icing thickness rates in the MARICE model using density of accreted ice, latent heat of fusion of pure ice, ratio of entrapped liquid mass to mass of ice accretion, thermal conductivity of water, freezing temperature of water film, water film thickness, specific heat capacity of water film, spray flux on freezing surface, spray temperature at generation, heat transfer coefficient at air-water interface, air temperature, thermal conductivity of water, liquid water content (LWC) [4]. The ICEMOD2 model presented by Horjen 2013 predicted the icing rate in terms of ice mass ($kg/m^2/s$) using wind speed (U_{10}), height above the mean sea level, significant wave height, vessel speed, relative wind heading, density of water, spray frequency, spray duration, and vessel direction with respect to waves as the main parameters [5]. Forest et.al. 2005, in the RIGICE04 model, predict the total ice accretion mass on offshore structures with variables including spray frequency, significant wave height, LWC, mass of water in one spray, height above the mean sea level, velocity of water droplets, spray duration, salinity, air temperature, sponginess of accreted ice, wind speed [6].

Laboratory setups favour controlled experiments and detailed measurements, but does not enable modelling of ship characteristics as wave generation, long spray flights with cooling of airborne spray droplets etc. Therefore, this experimental study was focused on basic fluid mechanics parameters and fluid properties governing sea spray icing, and what may be modelled and measured in the confined lab. These variables could be categorised into two categories: metocean parameters and parameters dependent on ship characteristics. The metocean parameters include *atmospheric temperature, sea temperature, wind speed, and salinity*. The parameters that are dependent on ship and wave characteristics include *spray flux, spray frequency and spray duration*. *Wind speed* may also be considered as a parameter depending on ship characteristics since the ship design and wind direction highly affects the near-surface wind conditions and cooling of the surface. Material was the lone parameter identified that is only ship/ structure specific.

Kulyakhtin 2011 has shown that changes in humidity inside a droplet cloud has no significant effect upon the droplet temperature [14]. Humidity was hence not considered as a variable. Most of the existing sea spray icing models mentioned above use droplet diameter as a variable. Ryerson 1995, measured the droplet size spectrum and the LWC close to the spray impact location on the 115m Coast Guard Cutter wherein 39 spray events were sampled [11]. It is difficult to determine if a spray generated due to the impact of any random vessel with waves would confirm with these spectra of droplet sizes from the observations from one ship. Researchers have investigated the use of mean volume diameter (MVD) as an estimation for the complete spectrum of droplet sizes, and Kulyakthin 2012 concluded that uncertainty in the spray MVD can result is errors of several orders of magnitude [15]. Therefore, the droplet size was not included in this study. However, the nozzle and pressure combinations were selected in the range of droplet sizes that were presented in previous research. Details of the selection of the nozzle are outlined in section 3.1.

3. Experimental Setup

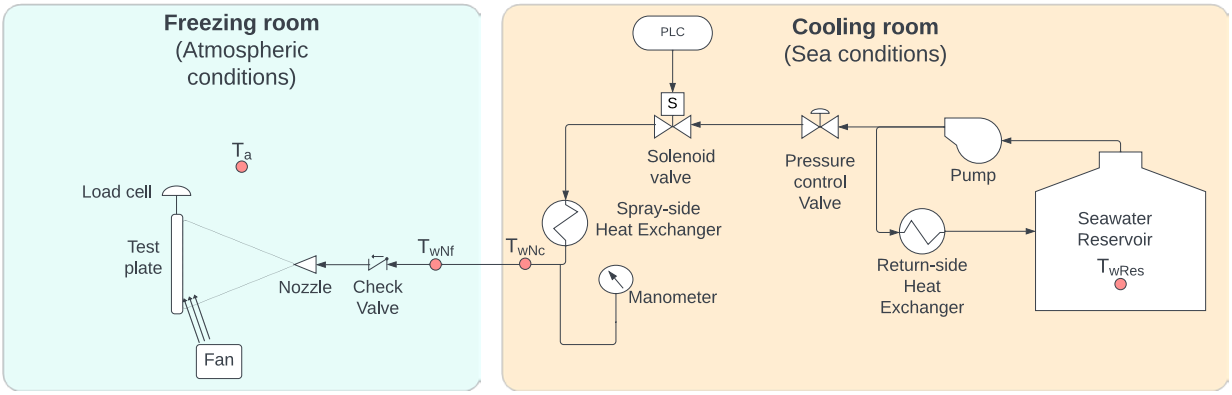

Figure 1: Schematic of experimental setup

The experimental setup consisted of 2 rooms. The first room (right side in Figure 1), called the 'cooling room', simulated the cold sea conditions and was set between +2°C and +6°C throughout all the experiments. The second room (left side in Figure 1), called the 'freezing room' simulated the freezing air conditions and was set between -15°C to -5°C depending on the experiments.

Seawater was stored in a 1000 litre reservoir in the cooling room. A pump was used to build up the flow in the system. Pressure in the system was measured about 1.5m before the nozzle and was controlled with the help of a control valve. A solenoid valve, controlled by a PLC (Programmable Logic Controller), was used to simulate periodic spray conditions. This helped to set the spray duration and period. A return pipe returned the seawater back to the reservoir from the pump since the pump was in continuous operation. Temperature measurement after the pump showed that there was a significant rise in the temperature of seawater at the output of the pump. A heat exchanger on the return side helped maintain the temperature of seawater in the reservoir. Another heat exchanger before the nozzle ensured that the seawater temperature through the nozzle was as close to the set water temperature in the room. The line then proceeded to the nozzle through a check valve in the freezing room. The intermittent spray conditions made in necessary to have a check valve to prevent air entering the system when the solenoid valve turned off, the absence of which resulted in reduction of flow through the nozzle over time. Finally, the freezing room had the test plate at a distance of 2 meters from the nozzle, on which the ice accretion was measured. The weight of ice was measured as a function of the output voltage from the load cell in a data logger. In addition to the schematic, there were numerous thermocouples that were strategically placed throughout the system and connected to the datalogger outside of both rooms.

Additionally, there was a cross-flow fan of a length greater than the plate to simulate near-surface wind. This fan was placed in close proximity to the plate in a manner that the whole plate was subjected to the airflow.

Figure 1 shows the schematic of the experimental setup and the images from the setup can be seen in Figure 2, Figure 3, and Figure 4.

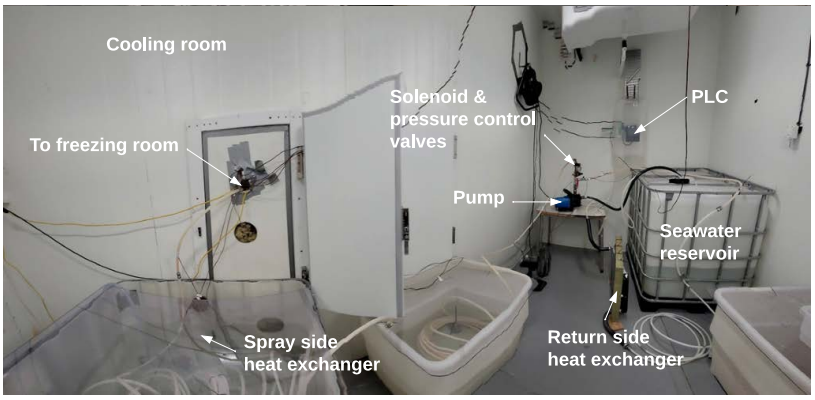

145

146 *Figure 2: Cooling room setup*

147

148 *Figure 3: Freezing room setup*

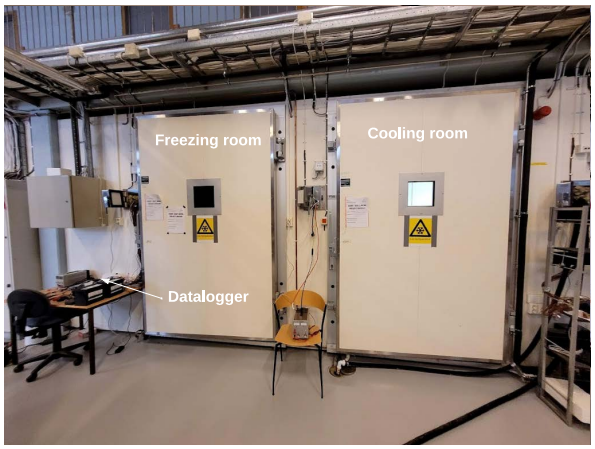

149

150 *Figure 4: Cold climate laboratory at UiT, The Arctic University of Norway - Campus Narvik*

3.1. Spray nozzle

Selection of the spray nozzle and operational pressure for experiments with sea spray icing controls droplet sizes, flow rate and distribution of the spray.

The experimental setup presented by Deghani-Sanij et.al., 2019 with respect to the nozzle, wind, and the plate, allowed for droplets that were only carried by the wind to impinge on the plate. In reality, there is a wide spectrum, of droplets within a spray cloud after interaction of a vessel with waves. Larger droplets tend to fall rapidly back in the water or in the forward part of the vessel whereas smaller droplets are carried by the wind to the aft part. The experiment used a nozzle and pressure combination that produced droplets of DV0.5 (Median Volume Diameter) approximately 975µm [13]. Droplets with diameters greater than 400µm are too large to be lifted by the turbulence [4], this value was however computed from wind generated spray. This could suggest that larger diameter droplets never reached the test plate, as it was not the momentum of the droplets, but the wind that carried the droplets to the plate. It is thus a possibility that the results of this experiment might be more useful for the aft regions of the ship than the forward regions since a CFD simulation by Kulyakhtin et.at. 2012 suggests a difference in the flow rate distribution of as much as $1x10^4$ between the forward and aft part of the ship [15].

Droplets of size 250 -500 µm are the primary reason for the spray flux at the aft, and sides of the vessel [2], this however depends on the size and design of the vessel. The nozzle used for the current experiments have a rated DV0.5 of 520µm ,410µm, and 350µm, at 1, 2, and 3 bars respectively. 3 bar pressure was the maximum that could be achieved with the available pump at the location of measurement (Figure 1). The nozzle was full-cone nozzle with a rated spray angle of 30°. Owing to the setup of the current experiment presented in Figure 1, most of the droplets within the full spectrum could be assumed to be impacting the plate due to the momentum of the particles exiting the nozzle.

4. Test structure

The test structure is presented in Table 1. The study comprised of 20 unique tests divided into 9 experiments. The first experiment, experiment 0, was conducted to study the repeatability of the tests under the same set conditions. The next 8 experiments with experiment numbers 1-8 are main experiments. In each experiment, 3 tests (4 in case of wind speed) were conducted by varying one variable while keeping the others constant. In each row in Table 1, the highlighted column shows the variable for the particular experiment.

Table 1: Experiment structure

Exp. Nr.	Constants / Varibles	Material	Wind speed (m/s)	Atmospheric temperature (°C)	Seawater temperature (°C)	Gauge Pressure (bar)	Spray duration (seconds)	Spray period (seconds)	Salinity (ppt)
0	**Repetition**	Aluminium	0 m/s	-9°C	+4°C	3 bar	0.25 s	9 s	32.45 ppt
1	**Material**	1. Aluminium 2. Steel 3. Fibreglass	0 m/s	-9°C	+4°C	3 bar	0.25 s	9 s	32.45 ppt
2	**Wind speed (m/s)**	Aluminium	1. 0 m/s 2. 2 m/s 3. 4 m/s 4. 6 m/s	-9°C	+4°C	3 bar	0.25 s	9 s	32.9 ppt
3	**Atmospheric temperature (°C)**	Aluminium	6 m/s	1. -5°C 2. -9°C 3. -15°C	+4°C	3 bar	0.25 s	9 s	32.9 ppt
4	**Seawater temperature (°C)**	Aluminium	6 m/s	-9°C	1. 2°C 2. 4°C 3. 6°C	3 bar	0.25 s	9 s	32.9 ppt
5	**Gauge Pressure (bar)**	Aluminium	6 m/s	-9°C	+4°C	1. 1 bar 2. 2 bar 3. 3 bar	0.25 s	9 s	32.9 ppt
6	**Spray duration (seconds)**	Aluminium	6 m/s	-9°C	+4°C	3 bar	1. 0.25 s 2. 0.5 s 3. 1 s	9 s	32.9 ppt
7	**Spray period (seconds)**	Aluminium	6 m/s	-9°C	+4°C	3 bar	0.25 s	1. 3 s 2. 6 s 3. 9 s	32.9 ppt
8	**Salinity (ppt)**	Aluminium	6 m/s	-9°C	+4°C	3 bar	0.25 s	9 s	1. 0.03 ppt 2. 32.45 ppt 3. 32.90 ppt

Some variables mentioned in Table 1 have underlying parameters that were the actual subjects of the test. The variation of the test plate material corresponds to the change in thermal conductivity and the change in pressure corresponds to the change in spray flux. The unit used for salinity is ppt (parts per thousand) which is the same as psu (practical salinity unit) used by oceanographers [16].

For all experiments, the distance between the nozzle and the plate, or the minimum spray flight distance, was constant at 2m. Video analysis showed that, in case of 3 bar pressure, the approximate flight time or the time required for the spray to reach the plate from the nozzle was 0.3 seconds giving an approximate ejection velocity of 6.66m/s. Atmospheric pressure measured inside the freezing room, located approximately at an altitude of 120m over the mean sea level, at -9°C with a multi-function ventilation meter was 97.5KPa. Changes in this value over the course of the study are not taken into consideration.

Some fluctuations were observed during the experiments. For example, the recorded temperatures showed slightly variation from the set temperatures and varied by about 1-2°C during each test due to the manner in which the refrigeration system controlled the temperature in the cold climate lab. This topic is discussed in detail in the results section for individual experiments.

5. Test procedure

The test procedure started with ensuring that the plate temperatures (using thermocouples glued in holes on the plate at a distance of 0.5mm from the surface facing the spray) and the water temperature in the reservoir were stable and as close to the set temperatures in the freezing room and the cooling room respectively. In addition, it was ensured that all other parameters are adjusted in accordance with the set test conditions. Recording the data logger was started. The pump was started at this point. The PLC was programmed to give a continuous spray for the first couple of minutes to ensure removing that all air pockets from the spray line. This ensured minimum variation of water exiting the nozzle throughout the experiment. During the initial continuous spray, there was a drainage system (Figure 5) that diverted the spray to the water collection tank and ensured that the spray does not come in contact with the plate.

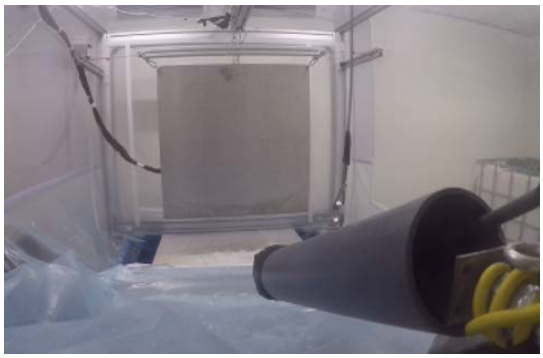

Figure 5: Spray drainage system

After the start of pulsating spray, the drain cover was removed with the help of a pulley mechanism. The pulley mechanism helped to remove the drain cover without entering the freezing room, without which, opening and closing of the freezing room resulted in excessive vibrations of the test plate, and thereby resulting in excessive noise in the weight data. This marked the start of the test period of 1 hour. The spray continued for exactly one hour, at the end of which, the pump was switched off. This marked the end of the test. The plate was allowed to rest for a few minutes to dampen the vibrations caused by the pulsating spray for recording the total ice weight (including ice stalactites under the plate). Next, the ice stalactites were scraped with a sharp metal plate, ensuring as close as possible, that no ice on the projected surface area of the plate was removed. The plate was again allowed to rest for some minutes for recording the reading of ice weight without the ice stalactites. This step marked the end of the test. Figure 8 provides details of the time intervals pertaining to the test.

6. Measurements and Data analysis

Table 2 presents a list of all variables used for the current study. It includes nomenclature, description, the source of measurement, and the formulae used for calculation, if any.

224

Table 2: Nomenclature & data source

Symbol	Unit of measurement	Description	Source of measurement	Formula/ Reference
u_{set}	m/s	set wind speed	hot wire anemometer	Figure 6
T_{aSet}	°C	set air temperature in freezing room	set in cold climate lab	-
T_{wSet}	°C	set seawater reservoir temperature (set air temperature in cooling room)	set in cold climate lab	-
p_{gauge}	bar	gauge pressure measured approximately 1.5 meters before the nozzle	manometer	-
t_s	sec	spray duration	set in PLC	-
t_p	sec	spray period or time between two consecutive sprays	set in PLC	-
T_{aMean}	°C	mean air temperature in freezing room for the duration of each test	thermocouple/ data logger	avg over 1 hour
T_{wRes}	°C	Temperature of seawater in reservoir	thermocouple/ data logger	-
T_{wNc}	°C	mean temperature of seawater measured before nozzle in cooling room for the duration of each test	thermocouple/ data logger	avg over 1 hour
T_{wNf}	°C	Mean temperature of seawater measured before nozzle in freezing room for the duration of each test	thermocouple/ data logger	avg over 1 hour
T_{wMean}	°C	Mean temperature of seawater out of nozzle	thermocouple/ data logger	$(T_{wNc+} T_{wNf})/2$
$\dot{m}_{plate}$	kg/hr	mass of seawater impinging the plate per hour	physical measurement	Figure 7
Q_{plate}	kg/m^2/hr	mass flux of seawater impinging the plate per hour	calculation	$(\dot{m}_{plate})/(A_p)$
s_{ppt}	ppt	salinity	Conductivity meter	-
ρ_i	kg/m^3	density of sea spray ice (assumed = 900 kg/m^3)	literature	[4], [17], [18]
A_p	m^2	surface area of each test plate (= 0.49m^2)	physical measurement	-
w_{ice15}	kg	total weight of ice in first 15 mins of test (from 10 min moving avg curve of ice weight)	Load cell/ data logger	Figure 9
w_{iceX15}	kg	total weight of ice excluding first 15 mins of test (from 10 min moving avg curve of ice weight)	Load cell/ data logger	Figure 9
w_{ice60}	kg	total weight of ice in 1 hour of the test (from 10 min moving avg curve of ice weight)	Load cell/ data logger	Figure 9
w_{tot}	kg	total weight of ice in 1 hour of the test (measured average after end of each test)	Load cell/ data logger	Figure 8
w_{plate}	kg	weight of ice in 1 hour of the test without ice stalactites (after scraping ice hanging below plate surface projected area) (measured average after end of each test)	Load cell/ data logger	Figure 8
r_{ice15}	kg/m^2/hr	effective icing rate for first 15 mins of each test	calculation	$w_{ice15}*4/A_p$
r_{iceX15}	kg/m^2/hr	effective icing rate excluding 15 mins of each test	calculation	$w_{iceX15}*(4/3)/A_p$
r_{ice60}	kg/m^2/hr	effective icing rate for each test calculated from 10 min moving avg of total ice weight	calculation	w_{ice15}/A_p
r_{tot}	kg/m^2/hr	effective icing rate for each test calculated from avg total ice weight measured after test	calculation	w_{tot}/A_p

r_{plate}	kg/m^2/hr	effective icing rate for each test calculated from avg ice weight without ice stalactites measured after test	calculation	w_{plate}/A_p
i_p	mm/hr	icing rate assuming uniform ice layer, calculated from ice weight without ice stalactites	calculation	$w_{plate}/A_p/\rho_i/1000$
i_{25}	mm/hr	icing rate considering all 25 points	physical measurement	Figure 11
i_{6-}	mm/hr	icing rate considering upper 6 points (low icing region)	physical measurement	Figure 11
i_{6+}	mm/hr	icing rate considering lower 6 points (heavy icing region)	physical measurement	Figure 11

Some measurements that do not have an obvious explanation in Table 2, are detailed out below.

6.1. Wind speed (u_{set})

A cross-flow fan of a length greater than the test plate was used to simulate the influence of wind on and near the freezing surface. The placement of the fan is shown in Figure 6.

The wind speed was measured with the help of a hot wire anemometer 9mm over the surface of the plate as shown in Figure 6. Wind speed was measured as an average of several readings at the top and the bottom of the plate. The difference in the wind speeds measured at the top and bottom varied by approximately 5% and was assumed constant over the entire surface of the plate.

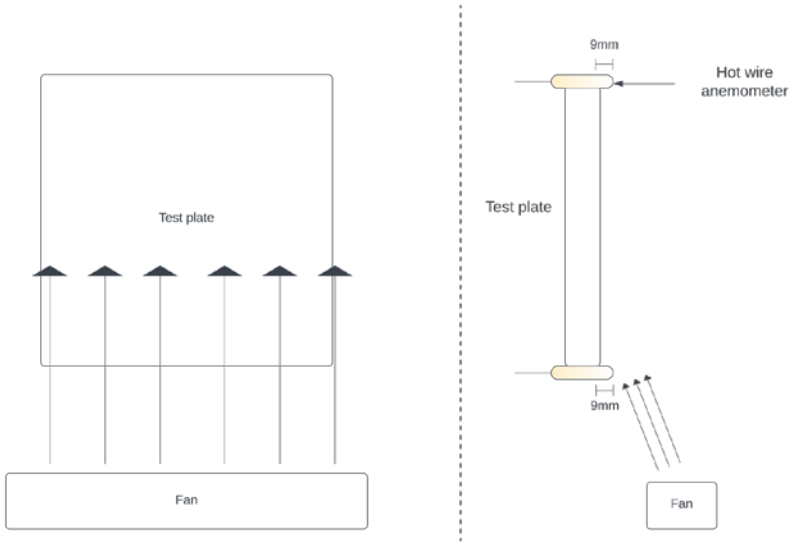

Figure 6: Schematic of windspeed measurement

The measurement of wind speeds in the experiment presented by Deghani-Sanij et.al., 2019 took place at a distance of 40cm from the fan, which was 2.1m from the plate, given that the distance between the fan and the test plate was 2.5m [13]. Wind speed measurements in the setup for the current study shown in Figure 6, were measured at the plate, which is a more accurate measurement for the wind speed affecting the freezing surface.

6.2. Temperatures

Temperatures were measured with the help of thermocouples and recorded every second with a datalogger. The locations of measuring probes for air and seawater temperatures are shown in Figure 1. The air temperature in the freezing room was monitored with a thermocouple suspended close to the setup, but away from the spray.

Temperature of seawater was monitored in the reservoir (T_{wRes}), but not used during the analysis owing to the rise in temperature due to the pump. Instead, seawater temperatures were measured close to the nozzle. The seawater temperature close to the nozzle was measured with a thermocouple inserted perpendicularly in the pipe, about 10cm upstream of the nozzle inside the freezing room (T_{wNf}). The intermittent stagnation of seawater in the freezing room due to periodic spray was expected to lower the seawater temperature out of the nozzle compared to the temperature of seawater in the reservoir. Thermocouple readings can be affected by radiation errors [19]. Since the pipe in this location was constantly exposed to the freezing temperatures, despite of the insulation, the readings for the sea temperature at the nozzle could have been lower than the actual values. Thus, another measurement of the seawater temperature was taken about 1.5m upstream of the nozzle, but this one in the cooling room (T_{wNc}). The actual temperature would lie somewhere in between the seawater temperature measured upstream of the nozzle in the freezing room (T_{wNf}) and the one measured upstream of the nozzle in the cooling room (T_{wNc}) and thus, the actual seawater temperature exiting the nozzle (T_{wMean}) was considered to be the average of these two readings.

6.3. Mass of seawater impinging the plate per hour ($\dot{m}_{plate}$)

The setup for measuring the mass of seawater impinging on the plate is shown in Figure 7. The setup was run for all combinations of the input variables (wind speeds, pressure, spray duration, spray period) used in the test, each for 15 minutes, with the first batch of seawater with 32.45ppt salinity. The setup consisted of a frame with inner dimensions of that of the test plate (0.7m x 0.7m). A plastic water retainer collected all the spray water and drained it through a hole at the bottom into a collection bin. The mass of water collected in a collection bin was measured. This mass was multiplied by 4 to give the mass per hour.

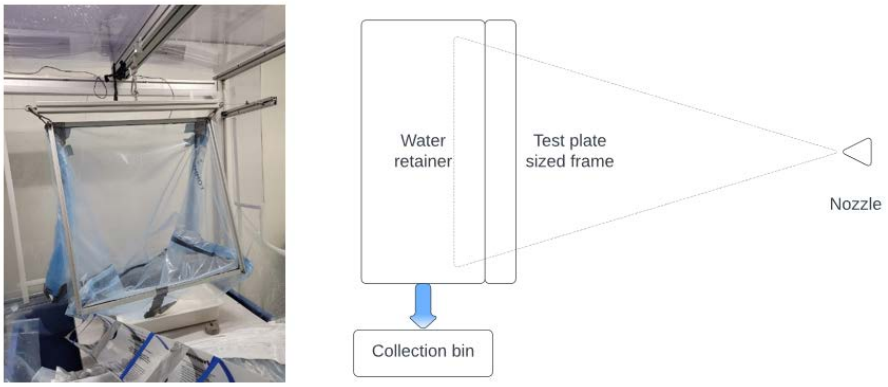

Figure 7: Setup and schematic for spray flux measurement

Measurements using the method used by Dehghani-Sanij et. al. 2018 to measure spray flux by collecting the water after hitting the plate in the small container [13], showed about 11.4% lesser flux than the current method shown in Figure 7. In the current method, 100% of the spray droplets that would have hit the plate are measured, whereas in the method described by Dehghani-Sanij et. al. 2018, some droplets that bounce back after hitting the plate are not captured, thus giving a lower value of flux than actually hits the plate. This difference in the measurement techniques is especially important due to the difference in the setup of the spray nozzle and the plate in both experiments (see Figure 1). In the experiment by Dehghani-Sanij et. Al. 2018, the nozzle was directed upwards, parallel to the plate, with a DV0.5 of 975µm, and the droplets that hit the plate were purely due to wind, and not the momentum of the droplets coming out of the nozzle. In section 3.1, it was suggested that it is possible that relatively larger droplets would be unable to be carried by the wind to the plate. This could have resulted in only the smaller droplets actually hitting the plate. In this case, the spray flux measurement technique applied by Dehghani-Sanij et. Al. 2018 would be valid, although, the results from such a setup would be more appropriate only for the aft parts of the vessel where the droplets might reach mainly due to being carried by the wind. In the setup for the current study, the spray nozzle faces the plate, thereby taking also the relatively larger droplets to the plate due to momentum. The flux measurement technique used in this case (Figure 7) is more appropriate for the current setup.

The tests were carried out with two samples of seawater and one of freshwater. Measurements for the mass of impinging seawater per hour ($\dot{m}_{plate}$) were done at ambient room temperature with the seawater sample with 32.45ppt salinity. Since the density of water changes with salinity and temperature, assuming the volume of water hitting the plate during measurements and the tests remaining constant, the percentage difference in $\dot{m}_{plate}$ during the measurements and the tests is solely due to the difference in the density. Table 3 shows how neglecting the changes in the density causes only a negligible error in $\dot{m}_{plate}$ of a maximum of 0.45% for both seawater samples and 1.54% for the sole test with freshwater. It is however to be noted that this applies only for the calculations of the mass flux and not the mass of accreted ice, since the mass of ice is directly measured with the help of a load cell. The densities in Table 3 are obtained from an open source density calculator [20].

Table 3: Density difference in various water samples

	Water sample	Salinity (ppt)	Approx. Temp.	Density (kg/m^3)	Error due to neglecting difference in density (%)
During Measurement of $\dot{m}_{plate}$	Sample 1	32.45	25°C	1015.63	-
During icing tests	Sample 1	32.45	2°C	1019.779	0.41
	Sample 2	32.895		1020.242	0.45
	Fresh water	0.03		999.992	-1.54

6.4. Weights from datalogger

The data logger registered the output voltage from the load cell throughout the duration of the whole test, in addition to some periods before and after the actual test duration. 11 calibration tests confirmed a 0.001mV/gm increase in the output voltage from the load cell. This calibration was used to calculate the ice weights from the raw data. A sample raw data from one of the tests is shown in Figure 8. To reduce the effects of the noise in the data, there were periods before and after the actual test duration for measuring weights. Before the actual test starts, there is a period to measure the average start weight of the plate. After the actual test duration, average weight is taken before and after scraping of ice stalactites, providing the basis for the calculation of w_{tot} and w_{plate} respectively.

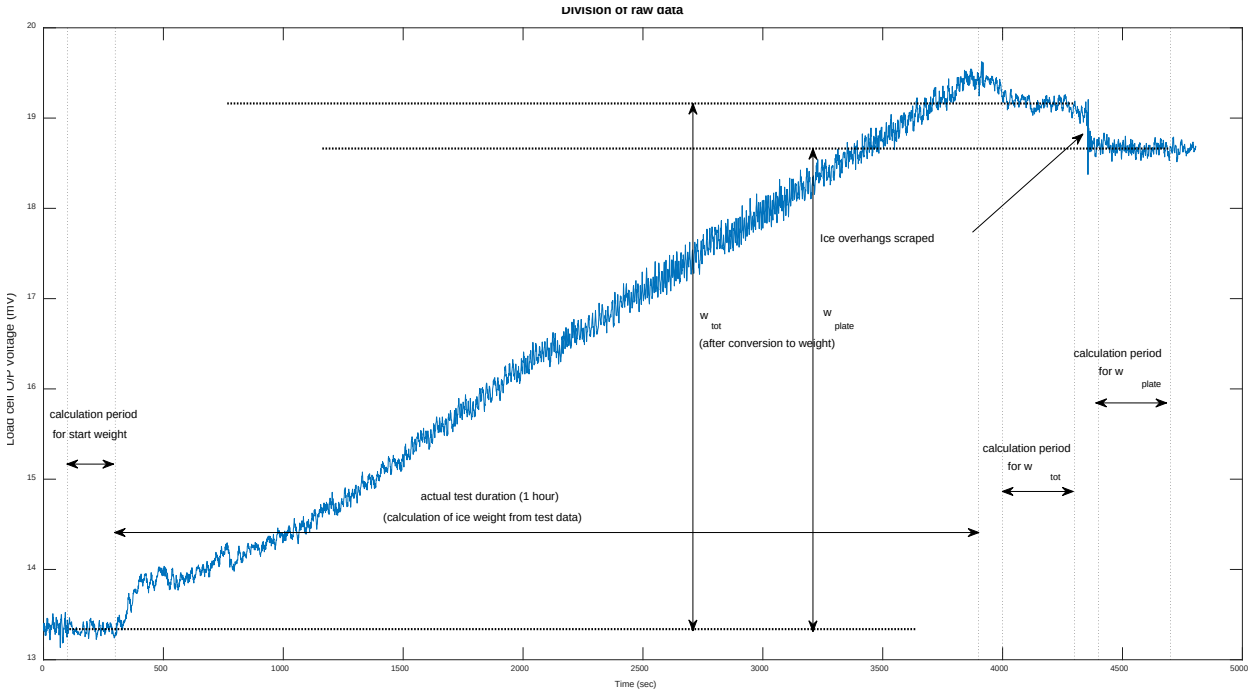

Figure 8: Timewise division of raw data from data logger (example of Experiment 7, test 1 with 3sec spray period)

Next, processing of the actual test data was carried out and is explained in the next section.

6.5. Data processing of weight measurements

Raw data for the actual test duration shown in Figure 8 was extracted and processed further to remove noise from the data. After experimenting with several curve smoothing algorithms and spans, it was concluded that the Robust Locally Weighted Scatterplot Smoothing (RLOWESS) algorithm [21] with a span of 600 timesteps (10 minutes) gave the bet fit for the raw data.

In Figure 9, the output voltage from the raw data is first converted to weight and then smoothed with the aforementioned function (blue curve). Due to the noise in the data, the start was not necessarily at 0gms. This data was then zero-adjusted, i.e., the start of this curve was moved to 0gms. The resulting red curve

in Figure 9 was considered to be the ice weight curve for individual tests. Figure 9 also shows the calculation procedure for the rest of the weights that were not covered in Figure 8.

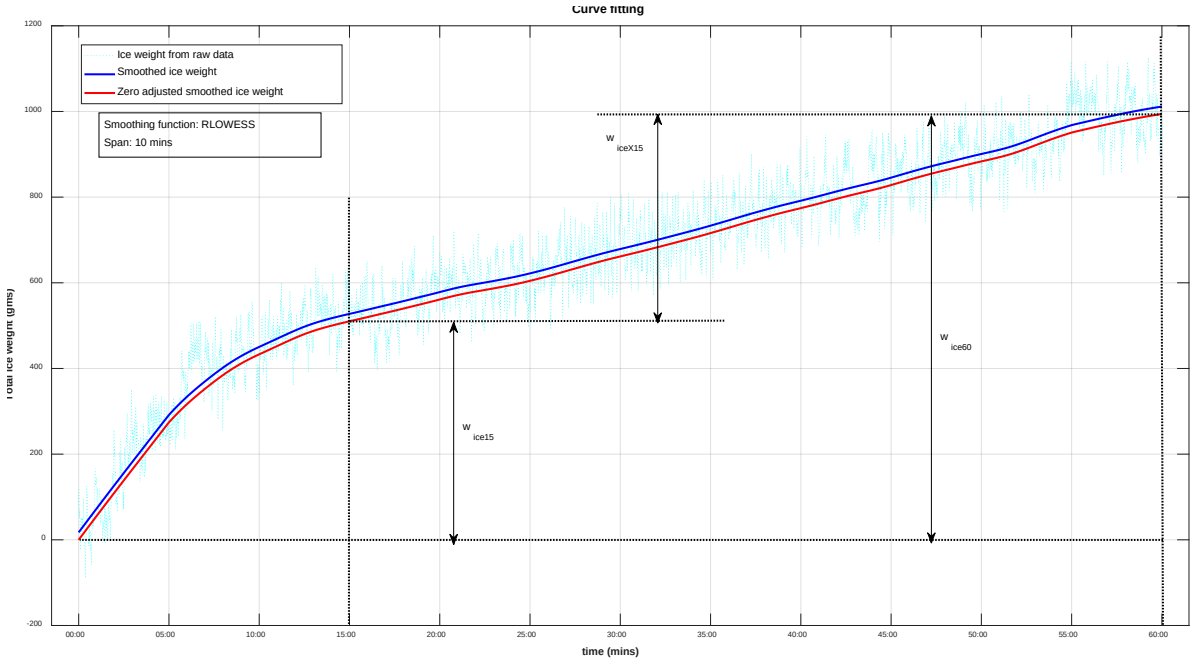

Figure 9: Noise reduction of weight data (example from experiment 2, test 1 for 0 wind speed)

Most calculations required the actual weight on the plate from Figure 9. However, it is the area density (mass per unit area) of ice accretion that is of more interest, for which another calculation was performed. As shown in Figure 10, the zero adjusted ice weight in grams from Figure 9 is first converted to kgs, and then, the mass per unit area is calculated by dividing this with the area of the plate. The icing rate is then calculated by taking the difference in the mass per unit area of consecutive points (per second) and converting the rate to per hour. Since the icing rate is calculated from the time averaged weight of ice accreted over 10 minutes, the icing rate too would be the time averaged icing rate over ten minutes.

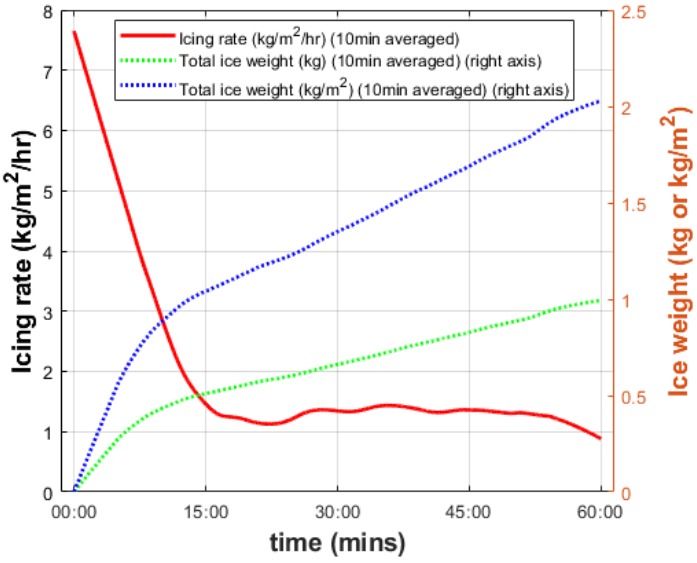

Figure 10: Calculating ice weight per unit area and time averaged icing rates.

6.6. Ice Weight measurements and icing rates

Figure 8 and Figure 9 show the 5 different weights measured for each test and Figure 10 shows the icing rate and ice weight per unit area calculated from the instantaneous total weight of ice on the plate. Most tests showed high icing rate in the initial stages of the test and that quickly declined to a near constant icing rate for the rest of the test. This is clearly spotted in Figure 10, where a knee-bend can be observed for the icing rate. It is later seen in 7.3 how this knee-bend is more visible for lower wind speeds. The reason for this is due to the difference in the thermal conductivities of the plate material and the ice layer and is explained in further detail in 7.2.

As shown in Table 4, r_{ice15} gives the effective icing rate for the first 15 minutes of the test. r_{iceX15} gives the effective icing rate excluding the first 15 minutes of the test. The knee-bend was observed at different times for different test conditions. The knee-bend that was furthest from the start was approximately at 15 minutes. Thus, it was decided to keep 15 minutes as the split time for all tests. Taking different initial time periods would obviously show a difference in the initial effective icing rates. w_{plate} gives the ice weight without ice stalactites after one hour. w_{ice60} and w_{tot} are the weight of total ice on the plate after one hour with ice stalactites. The difference is purely due to the difference in the methods of calculation as shown in Figure 8 and Figure 9. Icing rates (r) in kg/m^2/hr with corresponding prefixes are then calculated as shown in Table 2.

There is a reason for inclusion of all different measurements of icing rates in the analyses that can be attributed to the application. Knowledge about the development of the initial icing rate could prove to be applicable for anti-icing methods using heat, pulse heating, or vibration. Using icing rates that exclude the few initial minutes or those that consider the entire 60 min test duration could simplify long-term estimations for icing. Since the icing rates seem to be much higher in the initial stages of a maximum of 15 minutes, the effect of this high icing rate would disappear for longer test periods. In real conditions,

the mean duration for icing events is 15 hours with a standard duration of 13 hours [2], [22]. The icing rates with and without ice stalactites, again depend on the application. Estimation of ice accretion on large surfaces would require the icing rates without ice stalactites as the water forming the ice stalactites would flow to the next 'cell'. Icing rates with ice stalactites would be necessary for estimation of ice accretion where development of ice stalactites is a possibility. In the analyses for individual experiments, the 3 different icing rates after 60 minutes are visualised as an error bar, in Plot 3 of each experiment result figure, for example, in Figure 12 – Plot 3. The median of these 3 values is plotted, and the error bar shows the 2 extreme values.

6.7. Plate divisions and thickness measurements

Each of the 3 plates used in the experiments was divided into a grid of 25 divisions as shown in Figure 11. Since the plates were oriented vertically during the tests, icing observed in the lower parts was higher than that of the upper parts as the water film slides down due to gravity before freezing. This results in different icing rates in different regions on the plate. The icing rate measured by weight could not differentiate between the different regions. For determination of the icing rate by thickness however, at total of 75 measurements were done over the plate, 3 in each division with the depth probe of a vernier calliper. In case of very uneven ice build-up, the extremities or peaks were excluded, and the mean of multiple measurements was recorded for each of the 75 points. For measurements up to approximately 7-8mm of ice thickness with seawater, the probe could relatively easily pierce the ice. For larger thicknesses, holes had to be bored to take the thickness measurements. An ultrasonic thickness gauge proved of little help for measuring the ice thickness. The reason for this could have been air bubbles in the sea spray ice and the uneven nature of the ice layer that prevented good contact with the probe, in addition to the brine pockets. If using an ultrasonic thickness gauge, it is suggested that the ice surface be gently polished [23], for example, with the probe or a finger, to flatten out the surface. This method could be used if the ice surface is relatively smooth and the ice is without entrapped air bubbles.

4 different thickness measurements are presented in Plot 4 of all the experiments, for e.g., in Figure 12 – Plot 4. These include the mean of all 75 measurements in all 25 divisions of the whole plate, a mean of 18 measurements from each of the 6 divisions of the low icing region and the heavy icing region, and finally a thickness estimation assuming uniform ice layer, calculated from the weight of ice on the plate without ice stalactites (w_{plate}) assuming an ice density of 900 kg/m^3 [4]. Icing intensity is classified into slow, fast, and very fast icing depending on icing rates, which are <10, 10-30, and >30 mm/hr respectively [3], [24]. These intensities are indicated in the same plots.

It should be noted that the ice density was not measured during this experiment, and that literature provides different values of sea spray ice density. Ryerson and Gow, 2000 observed sea spray ice densities between 693-917 kg/m^3. Stallabrass, 1980 assumed an ice density of 890 kg/m^3 [9] ,whereas several other researchers assumed an ice density of 900 kg/m^3 [4], [17], [18] . The value of 900 kg/m^3 is used in the current article only for the purpose of calculation of icing rate assuming uniform ice layer, calculated from ice weight without ice stalactites (i_p).

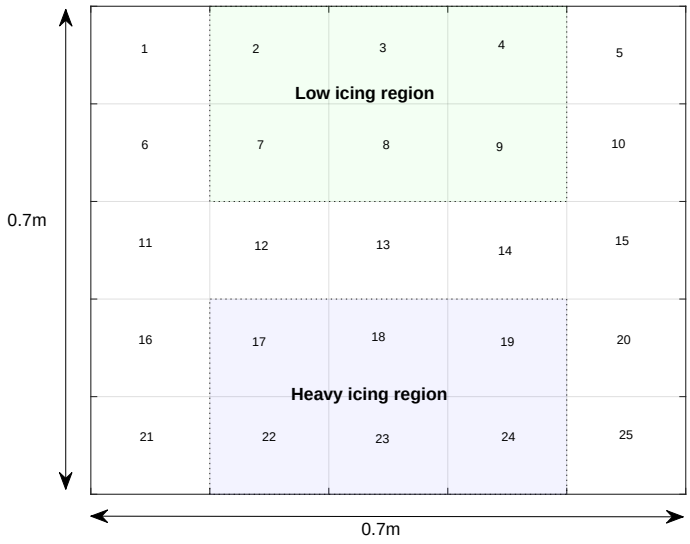

Figure 11: Plate divisions for thickness measurements

7. Results

7.1. Experiment 0: Repeatability

Repeatability is the precision of analytical measurements [25]. An ideal experiment has to be inherently repeatable. However, practically, some variables are difficult to hold constant throughout multiple readings. For testing the repeatability of the current study, 3 readings were taken in with the same set conditions. The measured air and seawater temperatures however, showed some variation. It is thus necessary to find out the amount of variation to be expected in a reading if taken multiple times. The repeatability was tested under one of the set conditions otherwise tested. The set conditions for Experiment 0 - the repeatability test are shown in Table 1 and the results are shown in Figure 12 and Table 4.

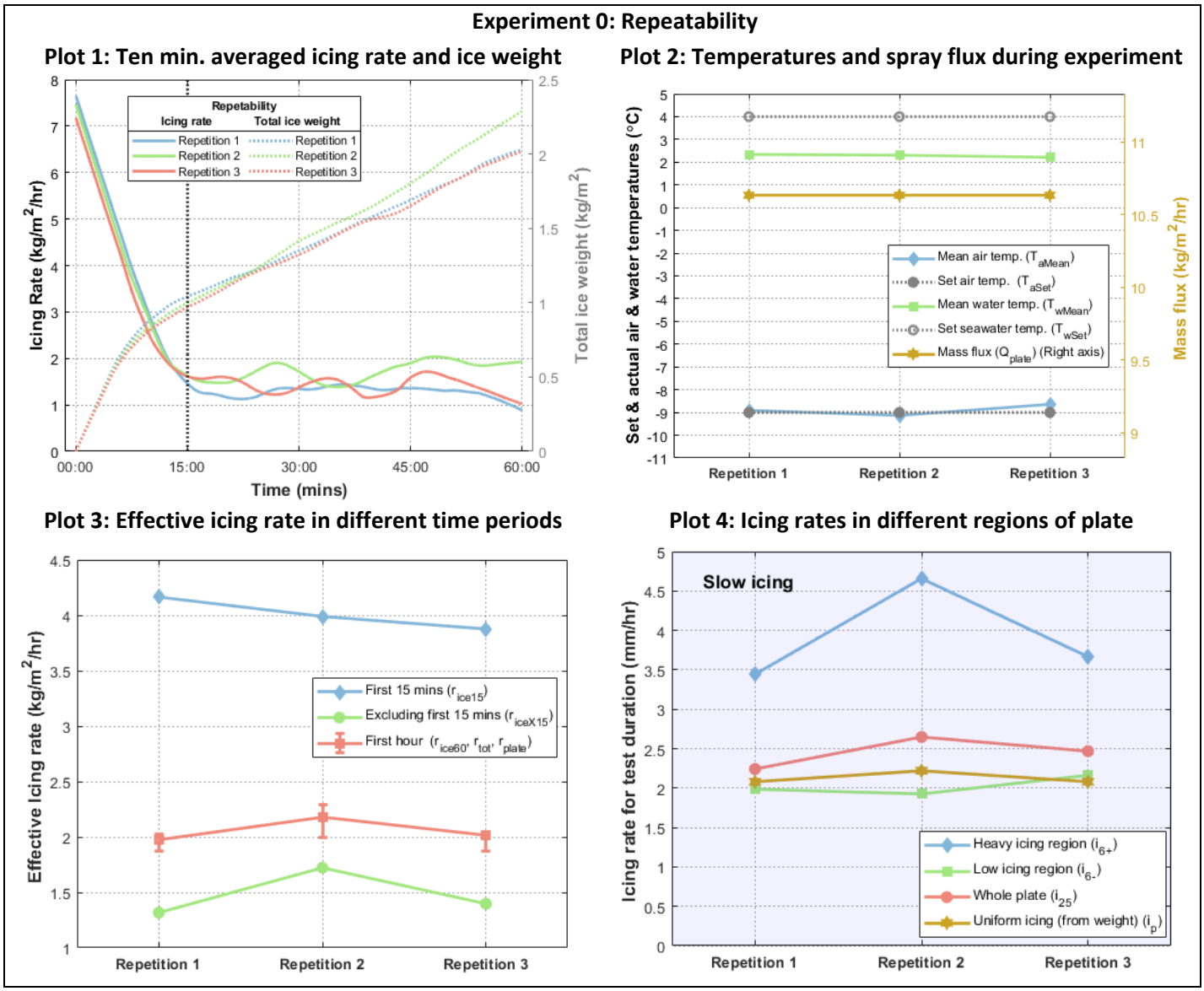

414 *Figure 12: Exp. 0 - Ice weights, temperature & spray flux variations, and icing rates for 3 repetitions with same set conditions.*

415 Figure 12 - Plot 1, shows the variation in the icing rates and the weight of accreted ice during the
416 duration of the three repetitions. Some variations, albeit minor, are visible from this figure. Figure 12 -
417 Plot 2 shows the variations in the mean of measured temperatures in each test. The mean air
418 temperatures show a small variation of less than a degree from the set temperatures. The seawater
419 temperature is about 2°C lower than the set water temperature for each test. Figure 12 – Plots 3 and 4
420 show minor variations also in the icing rates.

Table 4: Repeatability analysis (Exp. 0)

Test parameters												
Exp nr	Rep nr	Set Parameters								Measured values		
		material	u_{set}	T_{aSet}	T_{wSet}	p_{gauge}	t_s	t_p	s_{ppt}	T_{aMean}	T_{wMean}	Q_{plate}
		-	m/s	˚C	˚C	bar	sec	sec	gms/litre	˚C	˚C	kg/m²/hr
0	1	aluminium	0	-9	4	3	0.25	9	32.45	-8.91	2.34	10.63
0	2	aluminium	0	-9	4	3	0.25	9	32.45	-9.13	2.30	10.63
0	3	aluminium	0	-9	4	3	0.25	9	32.45	-8.64	2.21	10.63
								Mean		-8.89	2.29	
								Rel. Std. error (%)		8.02	1.25	

Test Results																
Exp nr	Rep nr	Ice Weights (kg)					Icing rates									
							by weight (kg/m2/hr)					by thickness (mm/hr)				
		From 10 min moving average			From end readings		From 10 min moving average			From end readings		assuming uniform ice layer	measured			
		w_{ice15}	w_{iceX15}	w_{ice60}	w_{tot}	w_{plate}	r_{ice15}	r_{iceX15}	r_{ice60}	r_{tot}	r_{plate}	i_p	i_{25}	i_{6-}	i_{6+}
0	1	0.51	0.48	0.99	0.97	0.92	4.16	1.32	2.03	1.97	1.87	2.08	2.24	1.99	3.44
0	2	0.49	0.63	1.12	1.07	0.98	3.99	1.72	2.29	2.18	2.00	2.22	2.65	1.93	4.66
0	3	0.47	0.51	0.99	0.99	0.92	3.88	1.40	2.02	2.01	1.87	2.08	2.47	2.16	3.67
				Mean			4.01	1.48	2.11	2.05	1.91	2.13	2.45	2.02	3.92
				Rel. Std. error (%)			6.84	10.11	7.24	5.08	3.35	3.72	9.60	5.81	30.48

The repeatability analysis is shown in Table 4 in terms of relative standard errors (RSE). The actual temperatures cannot be practically kept constant. The RSE in the air temperature was 8.02%, whereas the RSE in the seawater temperature was only 1.78%.

In case of icing rates by weight, the icing rate by weight excluding the first 15 minutes (r_{iceX15}) shows the greatest RSE at 10.11% and all other measures of the icing rates by weight have much lower RSEs.

In case of icing rates by thickness, the icing rates by thickness for the low icing region (i_{6-}) and that for the whole plate, either by measurement (i_{25}) or by weight measurements assuming a uniform icing layer (i_p) show RSEs under 10%. The icing rate by thickness in the heavy icing region of the plate (i_{6+}) however, shows a relatively high RSE of 30.48%.

Sea spray icing is a complex physical phenomenon having multiple independent variables. The experiment with the repetitions is just an example of how, even in controlled laboratory conditions, and the difference in the methods of measurement, there could be a variation in the recorded measurement of icing rates.

7.2. Experiment 1: Effect of material

Lightness, strength, and easy production make aluminium alloys one of the best choice for structures for several kinds of boats and vessels [26]. Construction of large scale container ships uses high strength and thick steel plates [27]. Fire retardant glass reinforced polyester (GRP) is used for construction of hulls and deck for totally enclosed type of lifeboats [28]. Depending on the possibility of procurement, the materials chosen for this study were aluminium alloy AL 5052, steel alloy S355 NVA/NVE, and GRP supplied by VikingNorsafe.

Al 5052 has a high corrosion resistance in marine atmospheres, and has a thermal conductivity of 138.4 W/m·K (W/m·°C) [29]. S355 has a thermal conductivity of 45 W/m·K [30]. Thermal conductivity of polymer resins and glass fibre typically lie in the range of 0.05-0.18 W/m·K and is dependent on several factors including composition [31], [32]. This value, compared to that of steel and aluminium is extremely small. The exact composition of the GRP plate was unknown, and its thermal conductivity was assumed to be 0.18 W/m·K. Thermal conductivity is also a function temperature, and all values mentioned in this section are for ambient room temperature.

Atmospheric icing research has shown that thermal conductivity of a substrate affects the dynamic ice accretion process significantly [33]. Other parameters such as surface coating and surface finish might significantly affect the icing rates [3]. The aluminium and steel plates used for this test were uncoated. For the purpose of this study, thermal conductivity is assumed to be the dominant parameter of differentiation between the materials and effects due to any other parameters are neglected.

This experiment (exp. 1) with thermal conductivity or material as the variable was conducted without wind. All the set input conditions for this experiment are listed in Table 1.

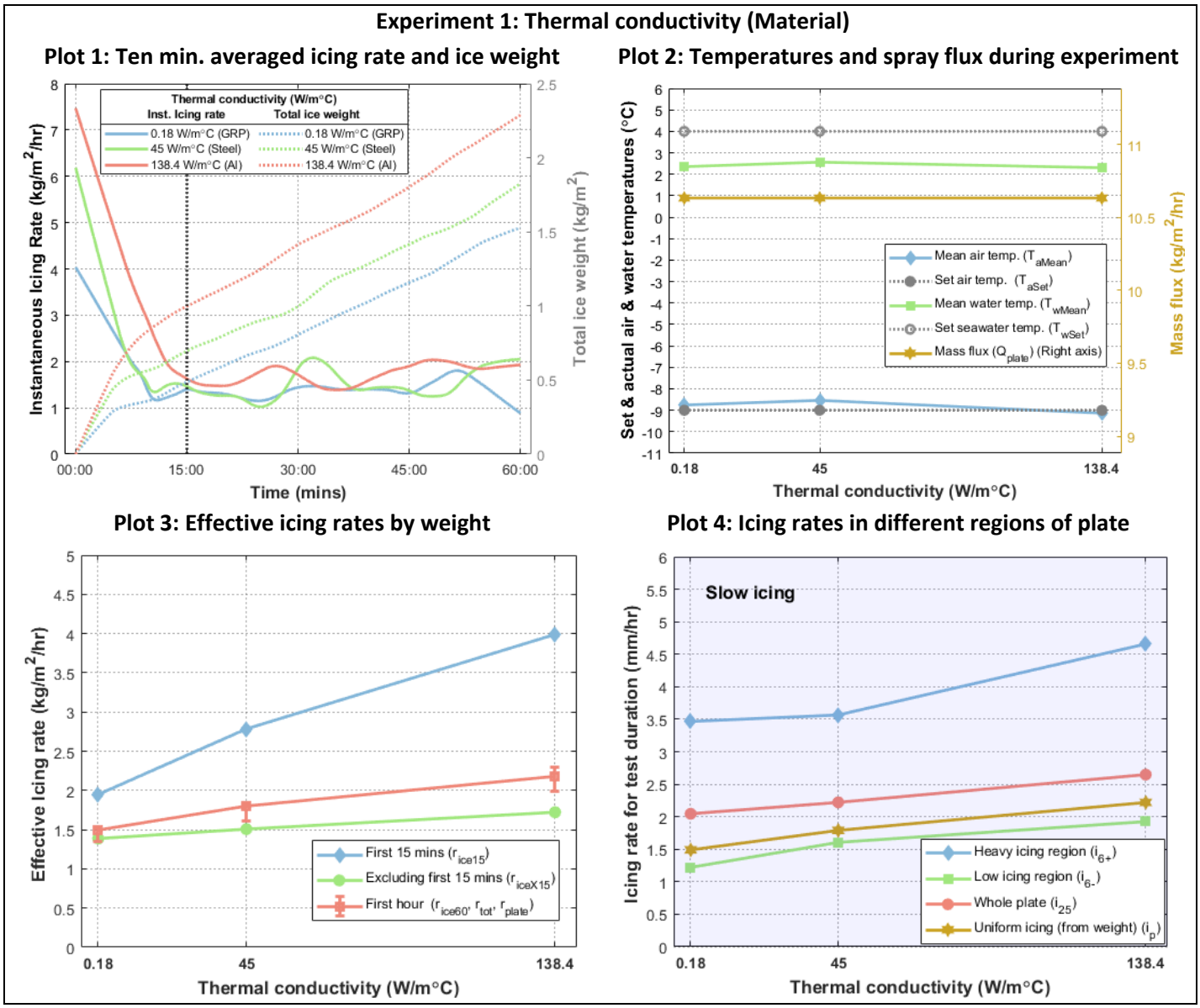

Figure 13: Exp. 1 - Ice weights, temperature & spray flux variations, and icing rates (Variable: Material)

Figure 13 – Plot 3 shows that the mean icing rates for the initial 15 minutes period vary greatly with the thermal conductivity. The Icing rates for the aluminium plate in the initial 15 minutes were close to twice that of the GRP plate. However, if the initial 15 minutes period is neglected, the icing rates have negligible variation with the material. This shows that the material plays an important role only during the initial icing phase, after which, the icing rates are more or less independent of the material of the substrate. This is in agreement to Kulyakhtin 2014, who stated that the average ice growth rate becomes constant after the first few sprays since the heat stored in the substrate is spent in the first few sprays and does not contribute in subsequent spray events [2]. Figure 13 – Plot 1 too, shows how, after 15 minutes, the icing rates for all materials are similar and the ice weight curves for all materials with respect to time are approximately parallel.

Owing to the lack of wind, all materials show slow icing intensity in Figure 13 – Plot 4, irrespective of the region on the plate. The icing thickness in all regions of the plate increases slightly with the increase in the thermal conductivity of the material. However, this increase is quite low. Since the ice thickness was measured only after the culmination of the tests, the icing rates by thickness for the first 15 minutes cannot be commented upon. It is however possible that the small difference in the icing rates by thickness at the end of 1 hour are a result of the unequal icing rates in the initial stage.

Figure 13 – Plot 2 shows that the average temperatures during all the tests in Exp. 1 were stable and deviated by less than a degree between all tests. The seawater temperature was more than a degree lower than the set seawater temperature for all tests.

Summary of results from Exp.1:

Experiment 1 investigates the variation in icing rate due to the material of the freezing surface. The experiment clearly shows that the icing rates in the initial few minutes are dependent on the material, more specifically, the thermal conductivity. As the ice layer builds up, the influence of the material on the icing rate is reduced. The initial ice layer itself insulates the freezing surface such that all materials become 'equal' in terms of further icing. For applications where the initial icing rates are important, for e.g., automation of anti-icing thermal cables, the material is definitely of consequence. In other cases, that require icing rates for a longer period of time, the influence of the material can be neglected as stated by Kulyakhtin 2014 [2].

The plate in the current experimental setup was not insulated, such that the temperature of the freezing surface on the side facing the spray were equal to the temperature at the rear at the start of the test. The temperature inside the hull of a vessel or inside a marine structure, or any other forms of heat sources close to the freezing surface would obviously affect the icing rate, especially in the early phase of the icing period.

7.3. Experiment 2: Effect of wind speed

Wind speed, or relative wind speed is one of the most significant factors contributing to sea spray icing [9]. Wind speed directly affects the evaporative heat transfer coefficient [7]. Higher wind speeds not only lead to faster in-flight cooling of the spray droplets, but also lead to faster freezing of the ice film. Previous research clearly shows that higher wind speeds lead to higher icing rates [8], [9], [15]. Especially during intermittent spray, higher wind speeds lead to faster freezing of the water film between the ice-air interface leading to higher icing rates.

Experiment 2 involved investigating the relation of icing rates to wind speed on and near the freezing surface. In the 4 tests in the experiment, the wind speed was varied for each test with all other parameters constant as shown in Table 1. Wind speeds were measured near the freezing surface as shown in Figure 6 and were varied from 0-6 m/s in steps of 2m/s. It should be noted that these are the equivalent of relative wind speeds and not the same as U_{10}, which is a standard for forecasting and metrological wind measurement. Relating this experiment to field conditions would require interpretation of these wind speeds in terms of U_{10} and the wind field near and around a ship or marine structure.

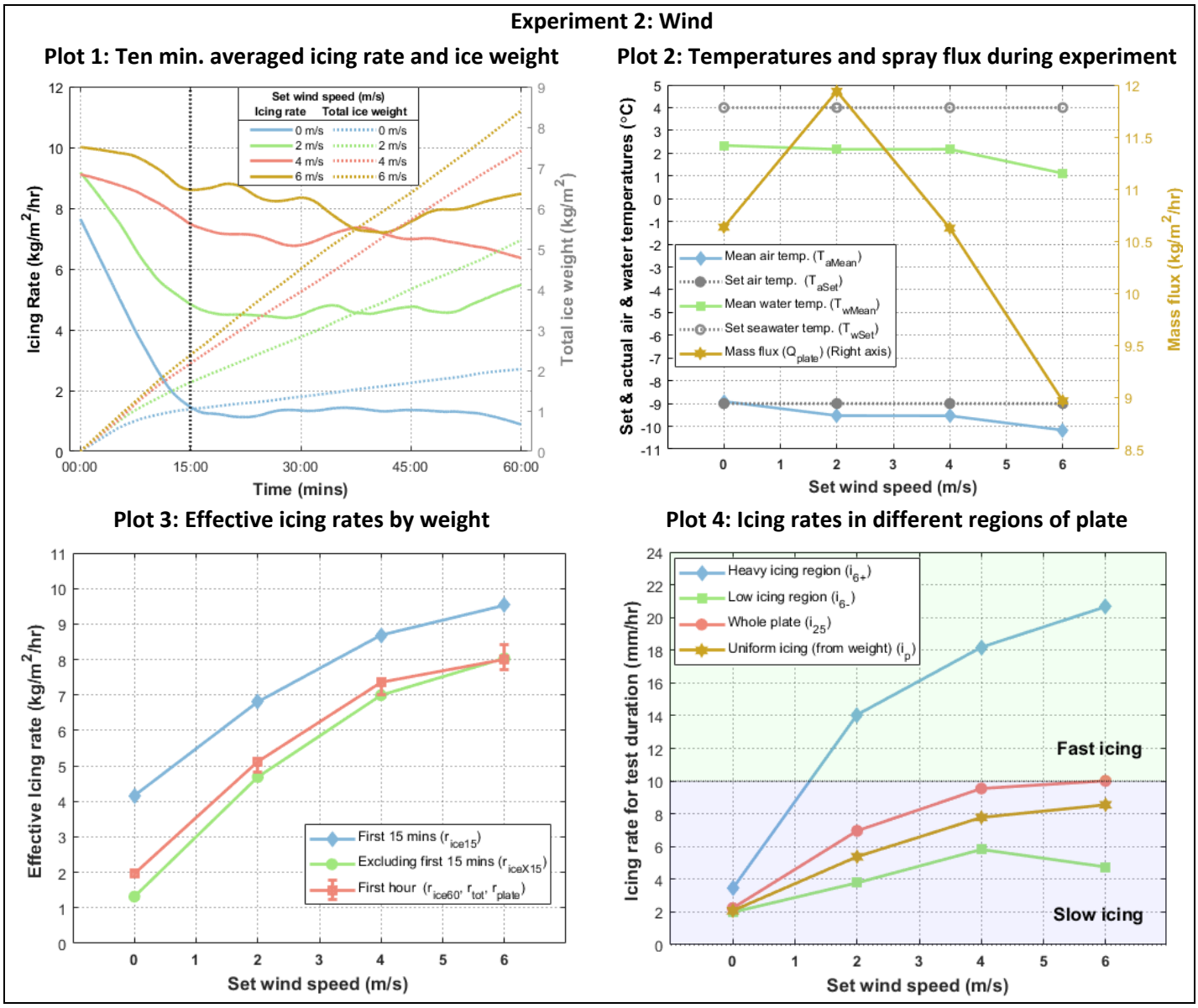

Figure 14: Exp. 2 - Ice weights, temperature & spray flux variations, and icing rates (Variable: wind speed)

Figure 14 – Plots 3 & 4 show how the icing rate increases with the increase in wind speeds. Figure 14 – Plot 3 shows that the icing rates for the first 15 minutes are higher than after the first 15 minutes. The difference however is reduced with increasing wind speeds. This means that as the wind speeds increase, the icing rate becomes less time dependent, at least for the first hour of icing. In case of no wind (which is a hypothetical icing case for field conditions), the rate of icing was 3.15 times higher in the first 15 minutes compared to after it, and 2.05 compared to the icing rate for the complete one hour (including the first 15 minutes), whereas, at 6m/s wind, the initial icing rate was just 1.19 times higher than that excluding the first 15 minutes.

As the wind speed increased from 2 to 6 m/s, the icing rate by weight increased from 5.11 to 8.01 kg/m^2/hr and that by thickness increased from 6.96 to 10.02 mm/hr for the entire plate, and 14.06 to 20.66 mm/hr for the heavy icing region.

Icing rate trends from both, Figure 14 – Plots 3 & 4, show that the change of icing rate with respect to wind speeds is reduced with increase in wind speeds. The icing rate is approaching a constant value at a certain threshold of wind speed.

Figure 14 – Plot 1 confirms this finding. It can be seen that the curves of icing rates and weights for higher wind speeds are closer to each other than the curves for lower wind speeds. From Figure 14 – Plot 1, it can also be seen that the difference in the icing rates in the initial stages, compared to the later stages, is higher for lower wind speeds. This difference is not as visible for higher wind speeds where the time dependence of wind speeds on icing rates becomes lesser. Since all experiments starting from experiment 3, are performed with a wind speed of 6m/s, this 'knee bend' that is seen for 0 and 2 m/s wind, would not be as prominent as in Plot 1 of Figure 12, Figure 13, and Figure 14.

The experimental setup did not allow for testing at higher near surface wind speeds than 6m/s, so the threshold of windspeed when the icing rate stops increasing remains to be found. It must also be considered that higher wind speeds will increase the inflight cooling of incoming spray.

Figure 14 – Plot 4 shows that the heavy icing region on the plate experiences fast-icing already at 2m/s wind. The mean icing rate for the entire plate, approaches fast icing for higher wind speeds. The local variation in the icing rates measured in mm/hr are dependent on the local flux on the freezing surface. Although the total mass flux across the plate surface was measured, the local flux at each of the 25 divisions on the plate was out of the measurement scope. In a way, this is analogous to field conditions where different regions on the ship will have different amounts on incoming spray leading to different icing conditions, but this is not a point of consideration for the current study.

Though the mass flux through the nozzle was constant throughout this experiment, the mass flux measured at the plate varied due to the wind affecting the flow of the droplets and driving some away from the plate. It is interesting to notice although the icing rate increased with wind speeds, Figure 14 – Plot 2 shows that the flux measured at the plate decreased with increase in wind. This means that the icing rates increased even though lesser water impinged on the plate. Due the variation of spray flux for different wind speeds, the flux acts as a covariate, and if ideally kept constant, could give a slightly different curve for the icing rates in Figure 14 – Plots 3 & 4. In ideal experimental conditions, the flux across the plate should remain constant despite of varying wind speeds. The drop in the icing rate in the low icing region for 6m/s wind could be attributed lesser spray reaching this region of the plate at higher wind speeds. Figure 14 – Plot 2 also shows that the experiments with the highest wind speed had lower mean air and seawater temperatures than the other tests. This might have resulted into an overestimation of icing rates at higher wind speeds.

Summary of results from Experiment 2:

Experiment 2 concerning relation between the icing rates and wind speeds gives a clear indication that the icing rates are highly dependent on wind speeds. For further analysis, the role of the covariates, i.e., the air and water temperatures, and especially the spray flux, needs to be evaluated.

The mean icing rate in terms of weight was almost 4 times higher at 6m/s wind than without wind. The icing rate in terms of thickness was approximately 5 times higher for 6m/s wind compared to no wind irrespective of the region on the plate. This confirms that wind plays a significant role in determining the icing rates due to sea spray icing.

7.4. Experiment 3: Effect of Air Temperature

Experiment 3 investigates the role of air temperature for sea spray icing rates. Along with wind speed, air temperature is one of the two most significant factors for determining icing severity [9]. Lower air temperatures lead to quicker freezing of the water film between sprays, leading to higher icing rates. Experiment 3 consisted of 3 tests at different set air temperatures, under the freezing temperature of -1.8°C at 32.9ppt salinity (Eq. (1)), with the other conditions constant as given in Table 1.

$$Freezing\ point\ of\ saline\ water = -0.002 - 0.0524 \cdot s_{ppt} - 6 \times 10^{-5} \cdot s_{ppt}^2 \quad \textit{Ref:}\ [9] \quad \textit{Eq. (1)}$$

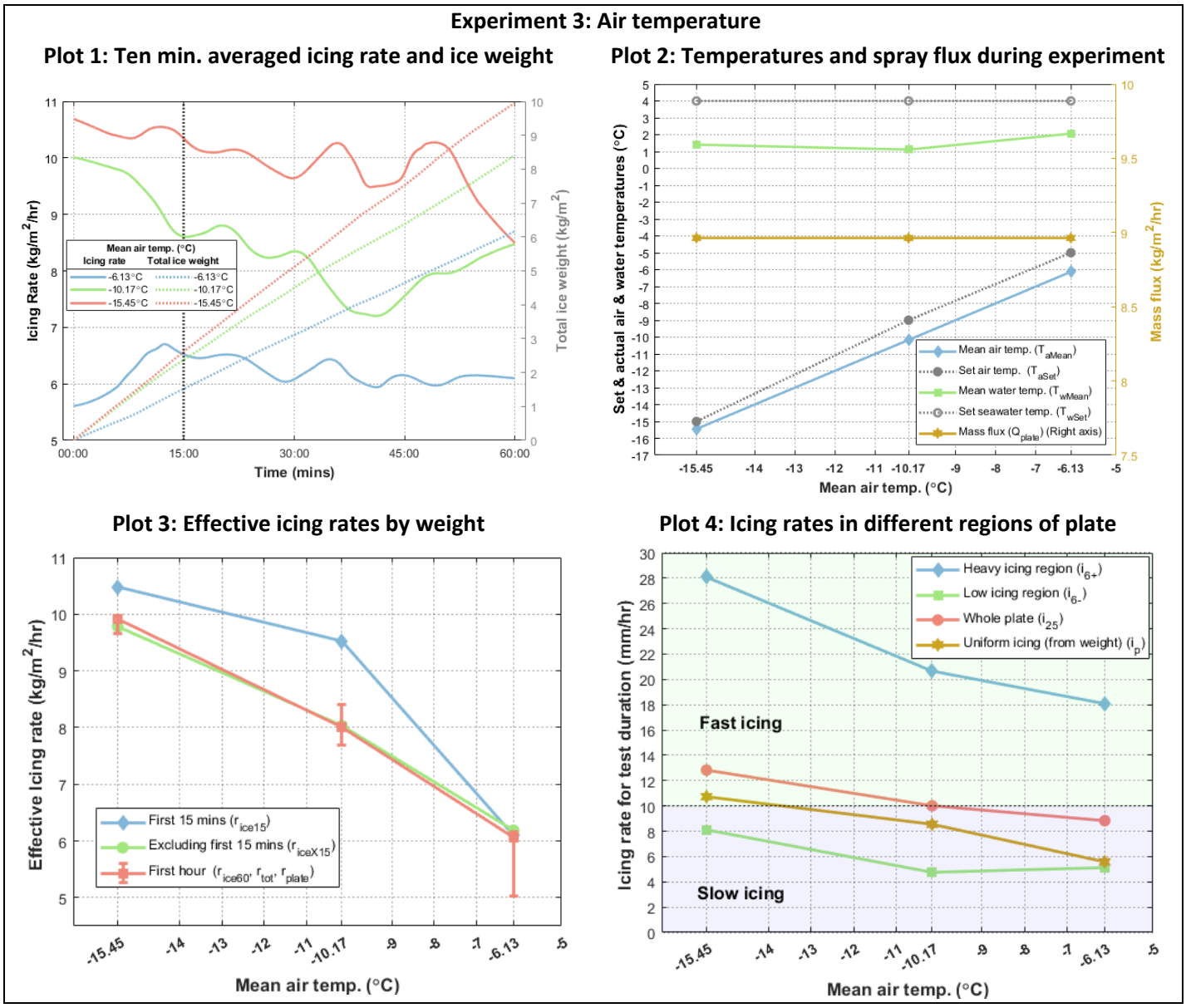

Figure 15: Exp. 3 - Ice weights, temperature & spray flux variations, and icing rates (Variable: Atmospheric temperature)

The three tests in this experiment were carried out at set air temperatures of -15°C, -9°C, and -5°C with recorded mean air temperatures of -15.45°C, -10.17°C, and -6.13°C respectively. Since this experiment focussed on air temperatures, for which the measured values were available throughout all the tests, the graphs in Figure 15, unlike the other experiments, are plotted against the measured mean air temperatures rather than the set air temperatures.

Figure 15 – Plots 3 & 4 show a clear trend where the icing rate increases with decrease in air temperature. Except for the initial 15 minutes, all measures of icing rates in terms of weight show almost a linear increase with the decrease in temperature for the range of temperatures tested. The icing rate in terms of weight increased from 6.06 kg/m^2/hr at a mean air temperature of -6.13°C to 9.92 kg/m^2/hr at -15.45°C corresponding to an increase of 0.41 kg/m^2/hr/°C fall in air temperature if linear relation is

assumed. The icing rates in terms of thickness increased by 4mm/hr for the entire plate, and 10mm/hr in the heavy icing region as the mean air temperature dropped from -6.13°C to -15.45°C.

There is only a small difference in the icing rates in the initial 15 mins as compared to the rest of the test for the tests with lower temperatures. This can also be confirmed from Figure 15 – Plots 1 where the deviations in the icing rates are comparatively low as compared to the experiment with wind at lower wind speeds.

In case of the icing rate in the first 15 minutes, the change of icing rate with temperature is higher for higher temperatures (from -6.13°C to -10.17°C) compared to lower temperatures (from -10.17°C to -15.45°C). The increase in icing rate due to air temperature is more or less linear if the first 15 minutes are neglected. The difference in the initial and overall icing rate in case of the highest temperature of -6.13°C however, is almost constant. Reasons for this could be that the marginal difference in the atmospheric temperature to that of the freezing temperature of seawater (4.33°C for the test with mean air temperature of -6.13°C) leads to slow freezing of the impacting seawater and might cause some of the accreted ice to melt in the initial stages when the ice layer is thin. The small difference in temperatures could also lead to lack of adhesion between the ice and the surface causing some of the ice sliding away due to weight in case of vertical surfaces. This was observed in case of the test with -6.13°C as shown in Figure 16. Plot 1 of Figure 15 also shows how, for the test with -6.13°C air temperature, the icing rate actually increases with time in the initial period.

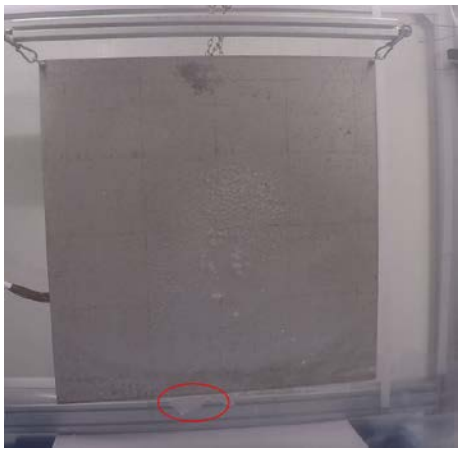

Figure 16: Breakup of initial ice layer at higher temperatures

Another important point to notice in Figure 15 – Plot 3 is that the icing rate in terms of weight has longer error bars for higher temperatures. As mentioned in 6.6, the error bar denotes difference in values due to difference in the interpretation of the weight of ice accreted. This means that the method of calculating the weight of ice accreted plays an important role for higher temperatures. The reason for this is that the formation of ice stalactites was more for higher temperatures. This was confirmed from the pictures from the tests shown in Figure 17.

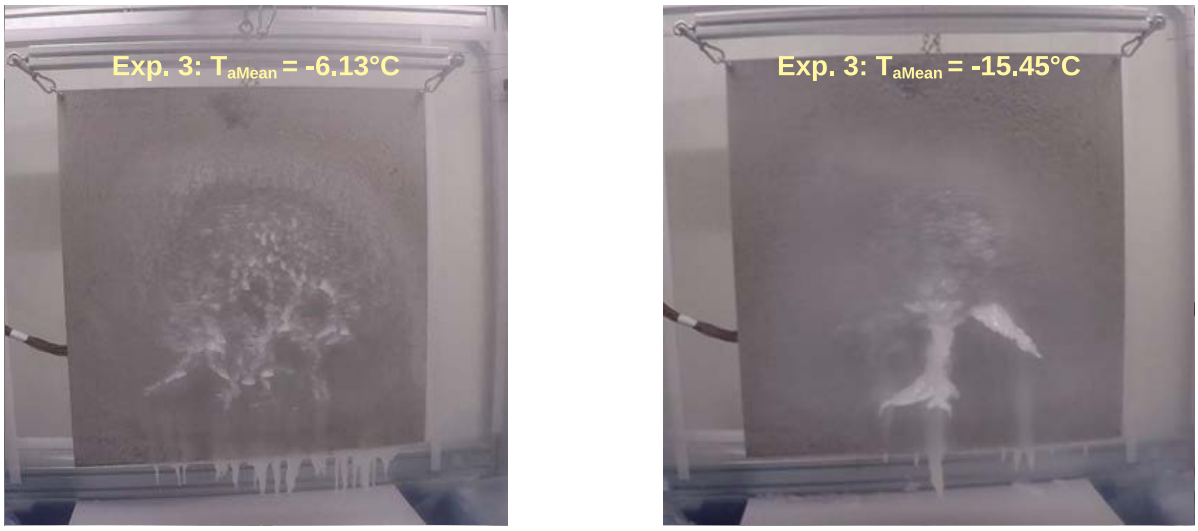

Figure 17: Testing effect of air temperature - More ice stalactites at higher air temperatures

Due to slower freezing for higher temperatures, a considerable amount of impacting spray water trickles down or 'runs off' before freezing, giving rise to more ice stalactites. Depending on the application, either the total weight of ice on the plate with the ice stalactites would be required, or in case a larger surface area is considered, the ice specifically on the projected area would be considered with the ice stalactites ice being a part of another 'cell' during the calculations. However, in case of larger surfaces the middle 'cells' will have a similar amount of water coming in from upper 'cells'.

Figure 15 – Plot 4 shows that the heavy icing region of the plate experiences fast icing rates for all temperatures. This is owing to the fact that the standard wind conditions throughout the experiment were of 6m/s. As the air temperature falls, it is seen that the mean icing rate for the entire plate too, experiences fast-icing.

Figure 15 – Plot 2 shows that the mean air temperature throughout the tests for higher air temperatures was at least a degree lower than the set temperature. This however has no implications on the results of this experiment since the results are reported at the actual mean air temperatures recorded during the individual tests. The seawater temperature was a bit higher for the test with -6.13°C air temperature than that of the other 2 readings, which could suggest some underestimation of the icing rates for this test at the given mean air temperature. All the 3 tests in this experiment had the same spray flux.

Summary of results from Experiment 3:

Atmospheric temperature is one of the most important factors in sea spray icing. The icing rates show a near linear increase due to the decrease in atmospheric temperature. The icing would start at a maximum temperature just lower than the freezing point of seawater, which depends on the salinity (-1.8°C for the salinity of 32.9ppt of the seawater used for this experiment). It was observed from the experiment that the icing rate increased by 0.41 kg/m^2/hr/°C fall in air temperature if linear relation is

assumed. In addition, at higher air temperatures close to the freezing point of seawater, freezing of the water film is slow. This leads to the impinged water trickling down at a higher rate then at lower air temperatures before it freezes. This showed an increase in ice stalactites i.e., more ice hanging below the plate. In certain situations where there is danger of falling ice, it could be said that the ice formed at temperatures closer to the freezing point pose a greater threat. This difference in the ice formed at lower and relatively higher freezing temperature also affects how the total mass of accreted ice is calculated. At temperatures closer to the freezing point, the total mass of ice on the projected surface area of the plate would be relatively lower than if the weight of the ice stalactites is included. This could prove to be important during ship stability calculations.

7.5. Exp. 4: Effect of Sea Temperature

Experiment 4 investigates the role of the surface sea temperature in sea spray icing. Sea temperatures are of moderate significance for sea spray icing [9]. It could be imagined that at constant atmospheric temperatures, lower sea temperatures lead to higher icing rates due to lesser time taken for the water film to freeze owing to lower difference in sea and atmospheric temperatures.

As shown in Figure 18 – Plot 2 (and Plot 2 for all other experiments), the seawater temperature was measured at 2 places, upstream of the nozzle, one in the freezing room, and one in the cooling room. The temperature had to be registered due to two practical difficulties in keeping the seawater temperature constant in the entire system; the first being the rise of temperature due to the pump, and the second being the periodic stagnation of the seawater in the line leading to the nozzle, in the freezing room (more in section 6.2).

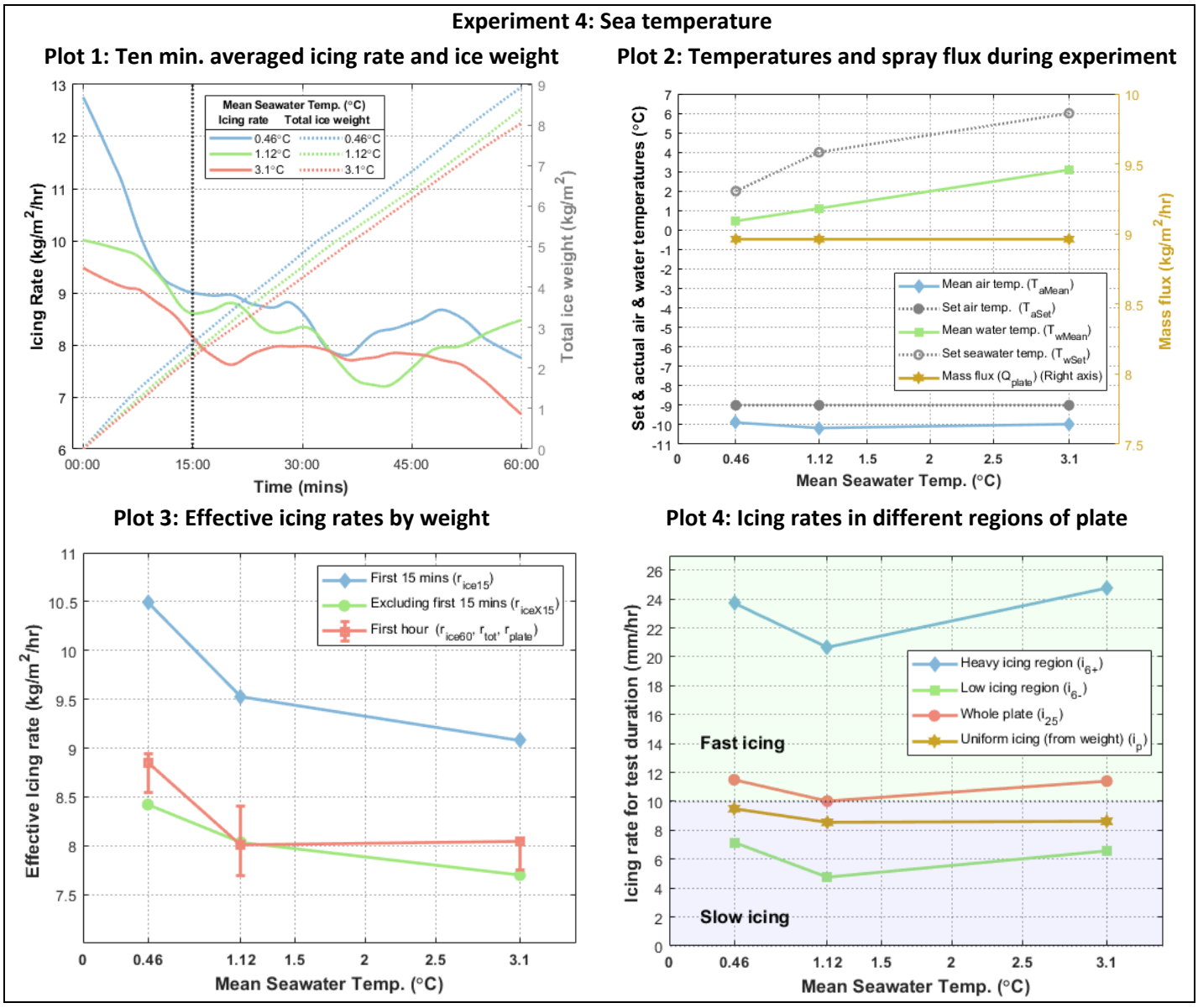

Figure 18: Exp. 4 - Ice weights, temperature & spray flux variations, and icing rates (Variable: Seawater temperature)

The three tests in this experiment were carried out at set seawater temperatures of 2°C, 4°C, and 6°C with recorded mean seawater temperatures of 0.46°C, 1.12°C, and 3.1°C respectively. Since this experiment focussed on seawater temperatures, for which the measured values were available throughout all the tests, the graphs in Figure 18, unlike the other experiments, are plotted against the measured mean seawater temperatures rather than the set seawater temperatures.

Figure 18- Plot 3 shows an increase in the icing rates for the first 15 minutes and the rest of 45 minutes of each test with decrease in seawater temperature. The absolute increase is however, small; 0.72 kg/m^2/hr for a 2.64°C drop in the set seawater temperature; showing that the sea temperature is not as significant as wind and atmospheric temperature in the sea spray icing process. This can also be seen in Figure 18- Plot 1, where the icing rates for all the three tests are very close to each other.

The icing thickness calculated from weight with an assumption of uniform icing over the entire plate shows an increasing trend in Figure 18- Plot 4. The values of all the different measurements of ice thickness differ with only 2-3 mm in corresponding regions over the complete range of seawater temperatures that are tested. It should be pointed out that the unconfirming trend of the physical mean thickness measurements could be a result of complexity for measurements due to uneven ice accretion as shown in Figure 17. This is the reason for inclusion of the data where uniform icing is assumed. In cases where the difference in icing rates does not significantly increase due to change in a certain variable, such as experiment 4, it could happen that the trends for measured ice thickness visible in the graph do not reflect the real trend due to either the practical difficulties in achieving ideal test conditions, or the random selection of points for thickness measurement within individual plate divisions.

The temperatures in Figure 18- Plot 2 show that the mean seawater temperatures were lower than the set seawater temperatures, as the setup did not allow for complete control over the seawater temperatures. This however has no implications on the results of this experiment since the results are reported at the actual mean seawater temperatures recorded during the individual tests.

Summary of results from Experiment 4:

Figure 18- Plot 3 shows a clear trend of higher icing rates with lower seawater temperatures. The difference between the icing rates over the range of mean seawater temperatures tested is, however, not as significant as due to the variation of wind and atmospheric temperatures. This confirms that the seawater temperature is only of moderate significance for sea spray icing.

7.6. Experiment 5: Effect of Spray flux

Depending on weather and spray parameters, ice accretion due to periodic sea spray icing may involve melting and freezing cycles. On each incoming spray in this case, the layer of ice at the ice-air interface melts due to the impinging seawater that is warmer than the ice. Freezing of this layer takes place in between 2 consecutive sprays [3]. The amount of seawater impinging on a freezing surface, i.e., the spray flux, directly affects the amount of ice accretion [34]. In general, the increase in the spray flux impinging on the plate increases the rate of icing up to a certain threshold of flux for the given conditions. However, over this threshold, it is possible that the incoming spray with a larger amount of water might melt or wash away some of the ice; the extreme condition of which is wave washing, where there is no ice accretion as the ice is mechanically removed by sea waves [4]. This suggests that the icing rate depends significantly on the incoming spray flux.

In experiment 5, the spray flux was varied by adjusting the pressure in the system with the control valve as shown in Figure 1. Each reading corresponds a gauge pressure of 1, 2, and 3 bars respectively measured approximately 1.5m before the nozzle. Finding the threshold of flux at which the icing rate falls was out of scope of the current experiment. Since the droplet size distribution through nozzles are dependent on pressure, this could be considered as another covariate in the experiment. The effect of droplet size is however not considered, rather, the selection of the nozzle is based on the droplet sizes used in previous literature (see section 3.1).

Studying the variation of icing rates due to change in the spray flux is also important since the flux was a covariate in several experiments in the current study due to the fact that the spray flux showed variation due to wind, spray duration, and spray period.

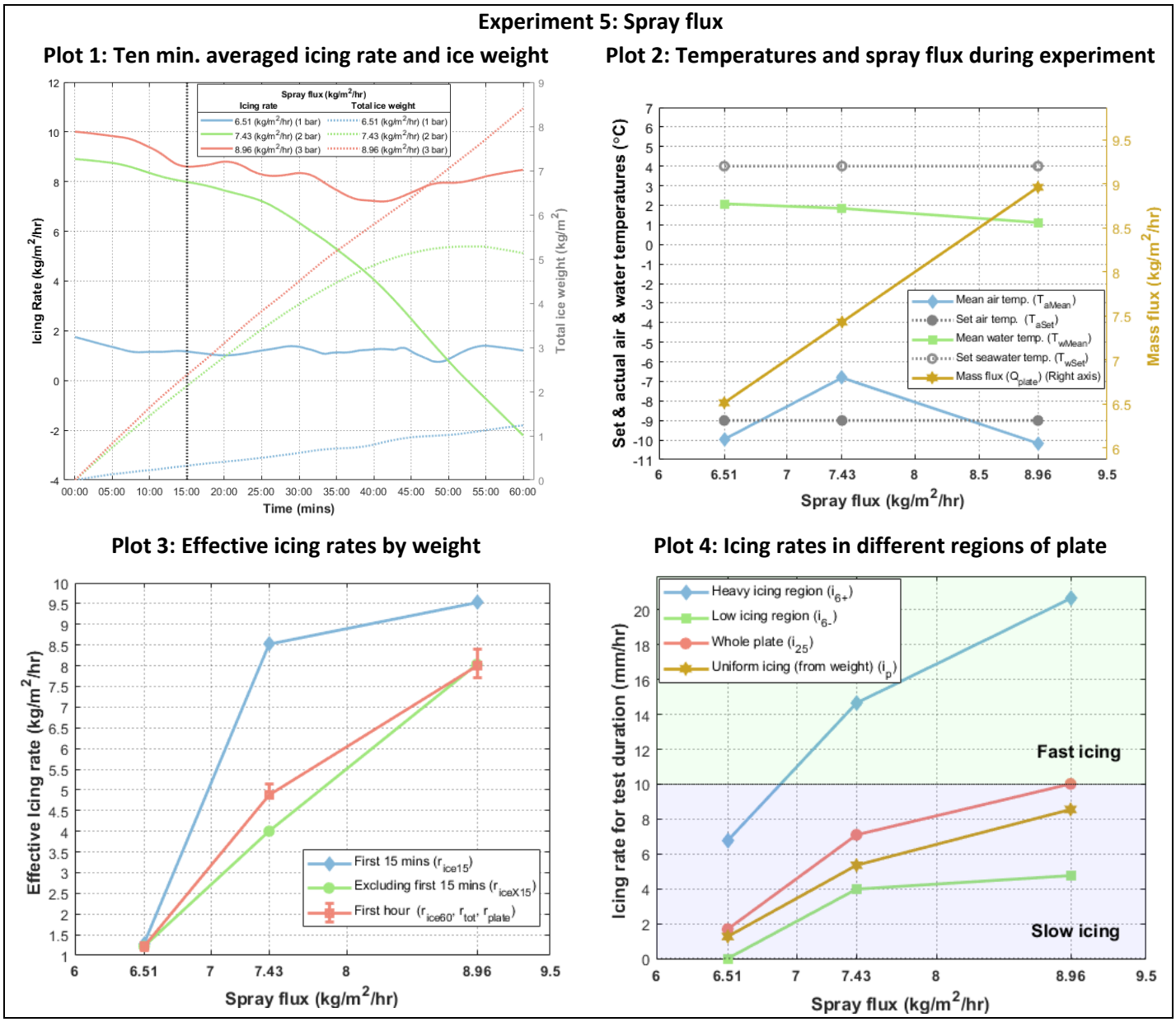

Figure 19: Exp. 5 - Ice weights, temperature & spray flux variations, and icing rates (Variable: Spray flux)

Figure 19 – Plots 3 & 4 show that the icing rate increases with the increase in spray flux. The icing rate by weight for the lowest flux at 1 bar pressure however was unexpectedly low. This could have been due to the fact that the low pressure of just 1 bar in the system did not carry the spray as well as in the other tests with 2 and 3 bars of pressure. This can also be seen in the value of icing rate by thickness that is zero in the low icing region for the test with the least spray flux. This would have led to severe underestimation of ice weights and thereby icing rate.

Additionally, Figure 19 – Plot 2 of the actual conditions in the experiment shows that the air temperature for the second reading was significantly higher than the set temperature. This suggests that the icing rates for this case might be underestimated. This can be an explanation of the dip in the icing rate towards the end of the second test with 2 bars of pressure and a flux of 7.43 kg/m^2/hr in Figure 19-Plot 1.

Summary of results from Experiment 5:

"When researchers selectively report significant positive results, and omit non-significant or negative results, the published literature skews in a particular direction. This is called 'reporting bias', and it can cause both casual readers and meta-analysts to develop an inaccurate understanding of the efficacy of an intervention." [35]

Except for the test with 3 bars of pressure with a flux of 8.96 kg/m^2/hr, the other two results are not reliable. The test with a pressure of 2 bars (flux of 7.43 kg/m^2/hr) showed an unexpected dip in the ice weight at the end of the test, the reason for which could not be pinpointed, but can be a result of the higher mean temperature in the freezing room. More importantly, the test with 1 bar pressure (flux of 6.51 kg/m^2/hr) did not seem to carry the spray well on to the plate. This could have resulted in false spray flux measurement since the entirety of the plate was not exposed to the spray and resulting into a severe underestimation of icing rate.

A suggested improvement while repeating this experiment would be to use higher pressures to vary the spray flux. This was unfortunately not possible for the current setup where a maximum of 3 bar pressure measured 1.5m before the nozzle.

Throughout the current study, there was an indirect variation in the spray flux due to other factors like wind, spray duration, and spray period in the other experiments. Analysis of the effect of the spray flux on icing rates could be done from these readings using statistical procedures.

7.7. Experiment 6: Effect of Spray Duration

Several existing sea spray icing models use the liquid water content (LWC) in kg/m^3 per spray as a variable for estimating icing rates [2], [7], [9]. It is a function of wave height, and researchers have presented various methods to estimate the LWC [6], [36]–[38]. The spray duration, along with the spray period, is dependent on wave and ship characteristics. Overland 1990, points out that icing forecasts provided by weather services is based on meteorological data, but for ship specific forecasts, the vessel length, wavelength, and wave height are all important factors [8].

The aim of having the spray duration as a variable is to investigate how the wave height (along with the wavelength and ship characteristics) play a role in sea spray icing. Although this analysis regarding the wave and ship characteristics is beyond the scope of the current study, experiment 6 investigates the direct relation of the spray duration with sea spray icing.

The spray duration and spray period are complex functions of factors including the wavelength, wave height, wind, ship characteristics, and sailing direction. In general, keeping the spray period constant and

increasing the spray duration gives less time for the water film to freeze before the arrival of the next spray. Since the spray frequency or period is kept constant in this experiment, the number of sprays per hour for all 3 tests are constant at 400 sprays/hour. This experiment assumes that the spray flux per hour would naturally increase owing to the increase in the spray duration of individual sprays. This causes the spray flux to be a covariate in the analysis for spray duration.

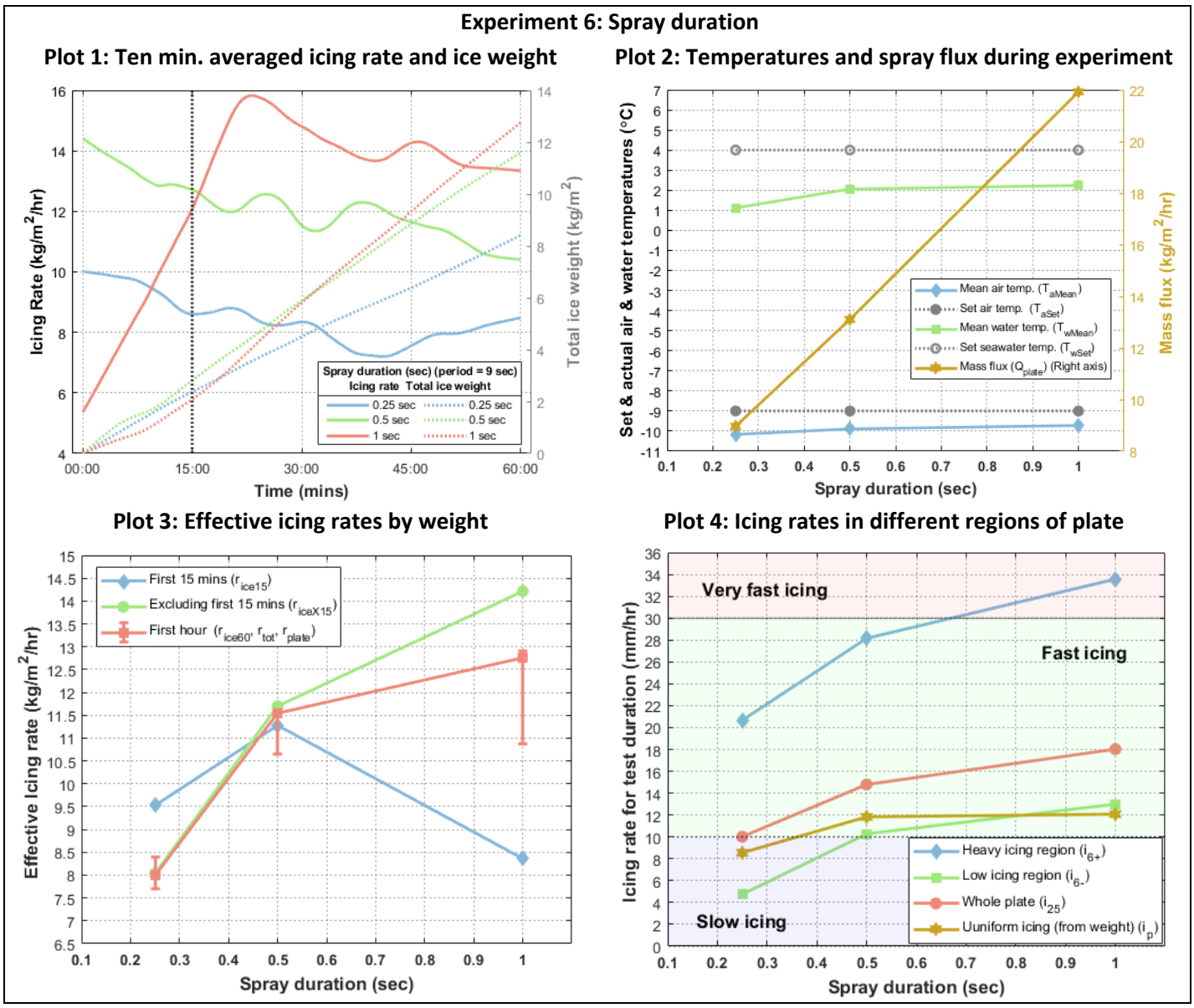

Figure 20: Exp. 6 - Ice weights, temperature & spray flux variations, and icing rates (Variable: Spray duration)

Figure 20 – Plot 3 shows that the mean icing rate recorded in the first 15 minutes goes up when the spray duration goes up from 0.25 seconds to 0.5 seconds. However, at a spray duration of 1 sec, the mean icing rate during the first 15 minutes falls significantly. Increasing the duration of spray adds more flux to the plate. The thin layer of ice formed at the start would be partially washed away due to the incoming spray. The icing rate for the remaining 45 minutes, however, suggests that once the initial ice layer builds

up, the icing rate increases much more than when the spray duration is small. This phenomenon can be observed in Figure 20 – Plot 1 where the icing rate for a spray duration of 1 second is the lowest at the start and steadily increases to a higher icing rate than the smaller spray durations. As seen in experiment 1, as the initial ice layers develop, the effect of the freezing surface on the icing rate decreases.

This is an example why it is important to study the icing rates also in the initial stages of icing. This difference between the initial and later icing rates could help to optimise anti-icing systems. To the best of authors' knowledge, none of the previous models have taken this difference in icing rates in the initial and latter stages of icing into consideration. However, as discussed earlier in experiment 1, when an icing event lasts for a relatively longer duration (several hours), the initial icing rate is of less importance.

The increasing error bars in Figure 20 – Plot 3 also suggest that there is a significant difference between the weights recorded with and without the ice stalactites. This in turn means that as the spray duration (and spray flux) increases, more water flows down and freezes below the projected area of the plate causing larger or more ice stalactites. As discussed earlier, although the ice stalactites can be said to be a part of the next lower 'cell' for calculations, in case of large surfaces, a similar amount water could be expected to enter from the upper 'cell' into the current one.

Figure 20 – Plot 4 for icing thickness rates show the heavy icing region of the plate experiencing 'Very fast icing' for a spray duration of 1 second. It is clear from Figure 20 – Plot 2 that the reason is the close to 2.5-fold increase in the spray flux compared to a spray duration of 0.25 sec. It is clear that the thickness of the accreted ice increases with the spray duration. It can also be noticed that the uniform icing thickness calculated from the weight over the entire plate not as high. This suggests that the icing becomes relatively more non-uniform as the spray duration increases.

Figure 20 – Plot 2 shows the significant increase in spray flux due to increase in the spray duration. To study the variation of icing rates due to change in spray duration, the flux ideally should have been kept constant throughout the experiment. Flux was something that was not directly controlled in the experiments, but changed primarily by changing the pressure in the system, and was further affected by wind. It was thus practically not possible to keep the flux constant. The average temperatures were a lower than the set temperatures indicating slight overestimation of the icing rates.

Summary of results from Experiment 6:

Though this experiment is aimed to study the dependence of icing rates on the spray duration, the significant difference in the spray flux makes it a significant covariate. Further investigation is necessary to form a conclusion about the dependence of the icing rates purely on the spray duration with a constant flux. If it is assumed that the flux would naturally increase as a result of increase in the spray duration, the test clearly shows higher icing rates for higher spray duration. This however would be true up to a certain threshold of spray duration, after which the rate of ice formation could slow down or eventually stop as the heat from incoming water limits the freezing of the water film on the plate. Analysing this threshold could be a suggestion for further research. Using the results for the spray duration for field estimations would necessitate interpretation of this data in terms of ship and wave characteristics.

7.8. Experiment 7: Effect of Spray Period/ Spray Frequency

Spray period is the time between two consecutive sprays. Spray period or spray frequency, just as spray duration, is a complex function of the ship characteristics and sea conditions. The frequency of spray impact on marine surfaces depends on the speed of the vessel relative to the wavelength and direction of the waves [10]. Overland, 1990 also suggests that the number of deck wettings, i.e., the frequency of spray is a function of significant wave height, speed of the vessel, and its length [8]. If the time between 2 consecutive spray events increases, the water film would get more time to freeze completely in between the 2 sprays. Since the spray period is changed, the number of sprays per hour changes for all the 3 tests in this experiment with 1200, 600, and 400 sprays per hour for spray periods of 3, 6, and 9 seconds respectively. Since the spray duration is kept constant, though the flux per spray is constant, the spray flux per hour for higher spray periods will naturally reduce due to the lesser number of sprays. This experiment assumes that the spray flux per hour would naturally decrease owing to the increase in the spray period or the time between 2 consecutive sprays. This causes the spray flux to be a covariate in the analysis for spray period.

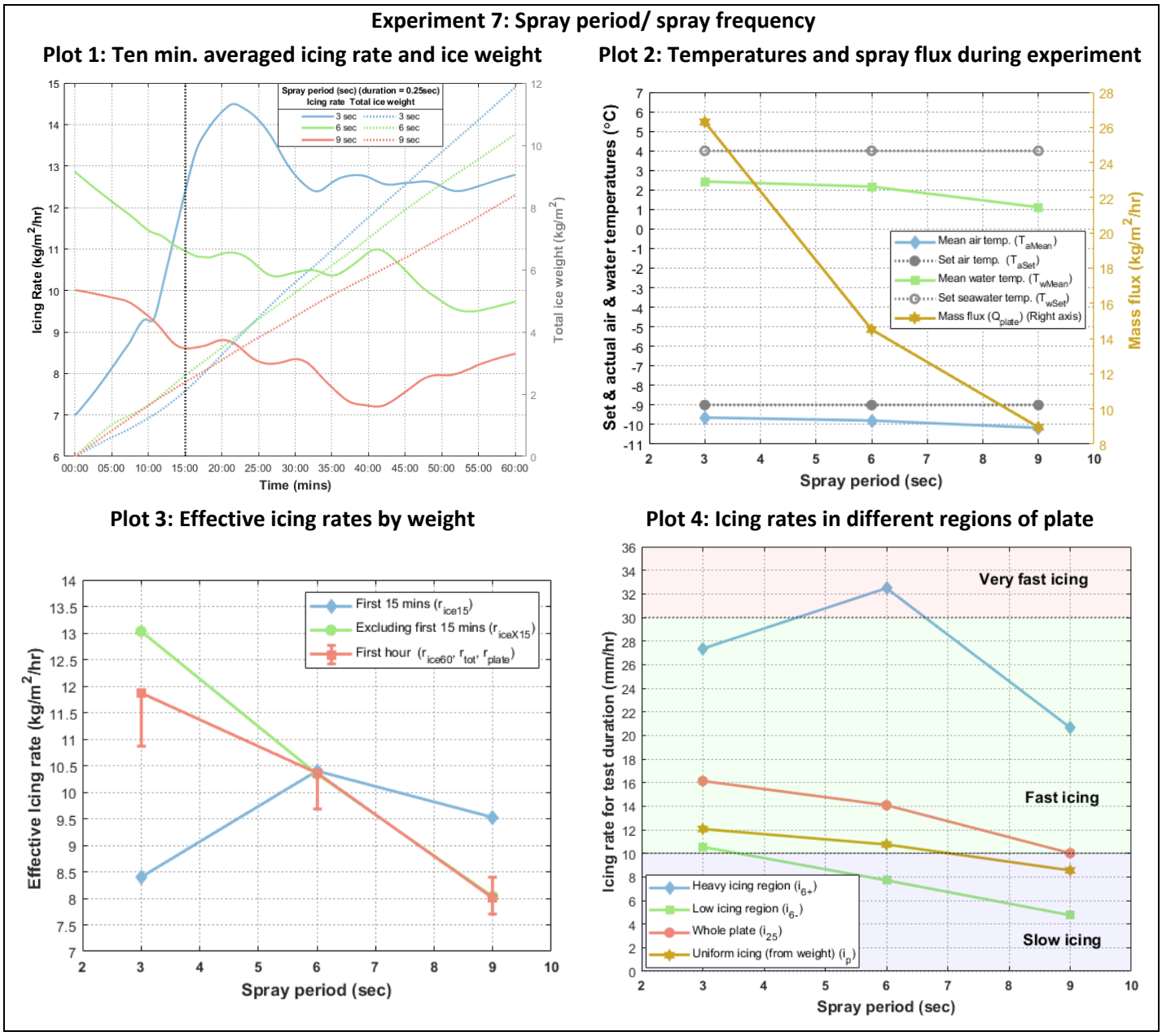

865 *Figure 21: Exp. 7 - Ice weights, temperature & spray flux variations, and icing rates (Variable: Spray period)*

866 Figure 21 – Plot 3 shows that as the spray period increases (as spray frequency decreases), the icing
867 rate in terms of weight decreases. This is a direct result of the decreasing spray flux on the plate per hour.
868 Figure 21 – Plot 2 shows the 3-fold decrease in the spray flux per hour as the spray period increases.

869 The icing rate in the first 15 minutes for a spray period of 3 seconds is much lower than in the latter
870 part of the test. The reason is similar to the case of higher spray duration in experiment 6. The water film
871 on the plate does not get enough time to freeze completely owing to the less time between incoming
872 sprays and thus keeping the surface relatively warm. However, after the formation of the first few layers
873 of ice, the ice keeps on growing rapidly. This too, as in case for experiment 6 with spray duration, can also

be observed in Figure 21 – Plot 1, where the icing rate for the spray period of 3 seconds is initially lower compared to higher spray periods, but eventually increases steadily to have the highest icing rate. As seen in experiment 1, as the initial ice layers develop, the effect of the freezing surface on the icing rate decreases.

Figure 21 – Plot 4 shows that the icing rate in terms of thickness decreases as the spray period increases, except for the heavy icing region. This could again be attributed to the decrease in spray flux. The ice thickness in the heavy icing region however shows an inconclusive trend. A closer look at Figure 21 – Plot 4 suggests that the difference between the icing rates by thickness in the low and heavy icing regions on the plate are smaller for a spray period of 3 seconds than larger spray periods. This could suggest relatively more even icing on the surface for more frequent sprays.

The seawater temperature measured at the nozzle in Figure 21 – Plot 2 shows a dip for the longer spray period of 9 seconds. This is because the water in the pipe towards the nozzle stays stationary for a longer time in the freezing room. This is an example of why the seawater temperature was recorded at multiple locations and measuring it close to the nozzle is important. Overall, all the readings had lower average temperatures for air and seawater than the set temperatures, suggesting that the icing rates could have been slightly overestimated.

Summary of results from Experiment 7:

Though this experiment is aimed to study the dependence of icing rates on the spray period, the significant difference in the spray flux per hour makes it a significant covariate. Further investigation is necessary to form a conclusion about the dependence of the icing rates purely on the spray duration with a constant flux. If it is assumed that the flux would naturally decrease as a result of decrease in the spray frequency, the test clearly shows higher icing rates for lower spray periods. This however would be true up to a certain minimum threshold of spray period, after which, more frequent sprays could slow down or eventually stop the ice formation as the heat from incoming water limits the freezing of the water film on the plate. Analysing this threshold could be a suggestion for further research. Using the results from the experiment with spray period for field estimations would necessitate interpretation of this data in terms of ship and wave characteristics.

7.9. Exp. 8: Effect of Salinity

To study the variation of icing rate to salinity, 3 tests were conducted in experiment 8. The first reading was taken with fresh water, the next with 2 different batches of seawater with a salinity of 32.45 and 32.90 ppt respectively.

Salts in supercooled sprays lower the nucleation temperature. Thus, increase in salinity lead to lesser icing rates [9]. Stallabrass, 1980 states that a small change in salinity of 5ppt results in variation of the freezing temperature by only 0.25°C; and is hardly of any practical significance for the severity of icing [9]. On the other hand, Kulyakhtin 2014 mentions how salinity plays an important role in ice accretion process at the water film level between consecutive sprays [4]. Kulyakhtin 2014 also mentions how wind generated spray has a significantly lower freezing temperature than seawater owing to higher salinity [4].

Since the freezing temperature, and thus the icing rate is affected by salinity, the experiment with differing values of salinity were performed. This experiment is especially important since multiple batches of saltwater were used for the entire study.

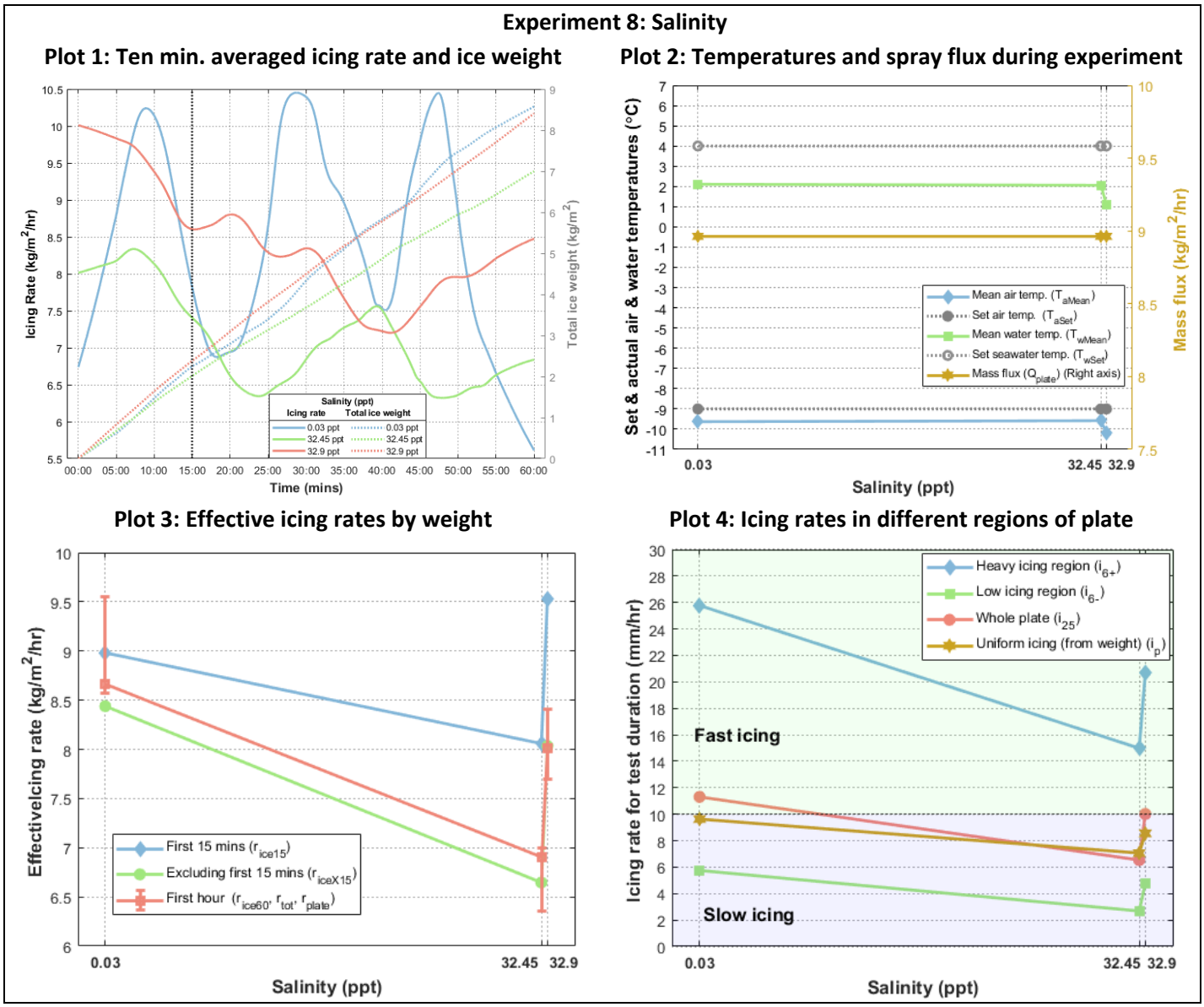

Figure 22: Ice weights, temperature & spray flux variations, and icing rates for Exp. 8 (Variable: Salinity)

Figure 22 shows that icing rates for freshwater and for 32.45ppt salinity in terms of both, thickness (Plot 4) and weight (Plot 3), as expected, go down for the test with seawater. It can also be seen in Figure 22 – Plot 2 that the mean temperatures for both tests are almost equal. However, in the last test with 32.90ppt salinity, the icing rates showed unexpected behaviour. The reason for the increase in the icing rates for this batch of seawater can be clearly seen in Figure 22 – Plot 2, which shows that the mean temperatures, both air, and water, during the experiment were close to 1°C lower than the first 2 readings. Figure 22 – Plot 4 shows that the significant dip in the temperature also caused the ice thickness to increase

significantly for the 32.9ppt salinity test. The air and seawater temperatures contribute to icing more than salinity, and thus the unexpected hop in the curve, also for the ice thickness. These temperatures act as significant covariates for this experiment.

Additionally, it is interesting to see that the icing rate with fresh water in Figure 22 – Plot 1 shows a strong periodic behaviour. Icing rate with fresh water depends purely on air and water temperatures with the other variables constant. The cooling mechanism of any refrigeration system holds the temperature between a certain upper and lower threshold of the set temperature. If the room temperature falls below the lower threshold, the refrigeration system stops and starts again only when the room temperature reaches the upper threshold – explaining the periodic appearance of the icing rate for fresh water. This cyclic nature of the refrigeration system does indeed also affect the icing rates for tests with sea water. However, the periodic appearance of the icing rates is not as prominent in case of saline water. This could be explained by the complex freezing process of periodic sea spray (saline water). At each incoming spray, salt exchange takes place between existing brine pockets and the newly formed brine film, and the freezing temperature of the brine changes due to salt rejection. This phenomenon can be said to dampen the effect of the periodic temperature change of the refrigeration system on the icing rates. This also shows that salinity indeed plays an important role in the calculation of icing rates for periodic sea spray icing.

Summary of results from Experiment 7:

Literature already suggests that higher salinity results in lower icing rates owing to lower freezing temperatures. This was observed from the first 2 readings of freshwater and 32.45ppt salinity. Analysis from the last test with a salinity of 32.9ppt showed lower mean temperatures of air and seawater during the test duration compared to the first 2 tests, and thus led to significantly higher icing rates. Significant variation in the temperatures for the tests make it difficult to reach a conclusion on the effect of salinity considering the effect of air and seawater temperatures on the icing rate is much greater in comparison.

8. Lessons learnt, summary, and future work

This paper presents results from a comprehensive experimental study of sea spray icing, including a detailed description of the experimental setup and lessons learned from the experimentation. Eight parameters governing the sea spray icing process were investigated experimentally. In particular, the initial stages of sea spray icing have been analysed and documented.

Sea spray icing is a complex process, and this also marked complexity under controlled laboratory conductions. Some of the general experiences and lessons learned from the experiments are listed below followed with a summary of observations from the results, and suggestions for future work.

8.1. Lessons learned

- Basis for the selection of the method of measurement of icing rate should be investigated and selected carefully. Variation in the method of measurement could lead to variation in the results. The weight of accreted ice can be measured with or without ice stalactites and could be used in

case of different applications. The weight measured by processing the raw data of the test duration and that which is measured after the duration of the test might show some variation depending on the data processing methods. If not presented as a range, and rather a single value, these variations should be accounted for in the errors.

- Icing rates in the initial stages of an icing event are generally higher than if the initial few sprays are neglected. None of the existing sea spray icing models account for this difference and neglect the higher icing rates at the start. Anti-icing methods requiring real time icing rates could make use of this difference in the icing rates for optimization purposes However, in other cases where long-term icing rates are applicable, the initial icing rates can be neglected. For general experiments with sea spray icing, it is suggested to report variation of icing rates with time.
- As sea temperature affects the icing rates, it is necessary to control and report the temperature of seawater during experiments. Internal heat generation in the pump significantly affects the temperatures of seawater, making it necessary for a heat exchanger between the pump and the nozzle, at least for a similar setup.
- Wind is a major factor affecting ice accretion. Measurements of wind speeds should be done as close as possible to the freezing surface or interpreted in such a manner so as to reflect the real wind speeds that act on the surface. Failing to do this would be a major source of error in the results.
- Because of how temperature control in refrigeration systems works, variations in the air temperature in cold climate laboratories cannot be avoided and the icing rates would have a certain dependence on these variations. This is a challenge for absolute repeatability of such experiments, and thus repeatability analysis should be reported.
- Air bubbles in the pipe leading to the nozzle proved to affect the flow rate through the nozzle. This is especially important while achieving periodic spray through mechanical means. It was experienced that as time progressed, the build-up of air bubbles caused the spray to be visibly weaker, within the 1-hour duration of the tests. This was tackled with the help of a check valve before the nozzle and ensuring the existing air pockets are removed by having continuous spray before the start of periodic spray, thus proving the spray drainage system in Figure 5 to be quite important.

8.2. Summary of observations from the results:

- Material: The material of the test plate affected the initial icing rates, but after some initial sprays, the difference in the icing rates was not significant. This means that for applications such as anti-icing with heating where the heat energy needs to be sufficient to avoid icing at all, information of the initial icing rates in the given condition could be used to optimise the heating systems such that the heat energy is enough to avoid any ice accretion. Whereas in cases where, for example, the total weight of ice accretion is required, the initial icing rates can be ignored since they are applicable only for the first few sprays.
- Wind speed: As expected, the icing rates varied greatly with wind speeds. Increase in wind speed caused increase in the icing rate. The increase in the icing rate for unit increase in wind speed decreases with increase in wind speed. This points to a threshold of windspeed after which the

icing rate would not considerably increase. Finding the threshold was out of scope for the current study. Though other variables were constant, the wind resulted in change in spray flux at the plate. The flux was thus a covariate and the reported icing rates are not purely for wind alone and further analysis of the data is required.

- Air temperature: Decrease in the air temperatures caused significant near-linear increase in the icing rates for the tested temperature range. At higher temperatures below the freezing point for a given salinity, more ice stalactites could be expected. Air temperatures were recorded for every second during the one-hour tests and showed fluctuations that could have affected the icing rates. The mean air temperatures during each test are reported, but the effect of instantaneous variations in the air temperature could be studied further from the data. Higher air temperatures resulted in more stalactites.
- Sea temperature: Icing rates increased with decrease in seawater temperature almost linearly. The variation was not as significant as due to air temperature and wind speed. The seawater temperature showed some amount of fluctuation during the tests. This too, like air temperature was recorded for ever second of the test. The seawater temperature showed only a moderate effect on the icing rates, and the instantaneous fluctuations could be considered to not affect the icing rate as much as the air temperature.
- Spray flux: Results from the experiment with spray flux as the variable was deemed to be not useful due to weak spray at lower pressures. The selection of the pump and piping is suggested to be improved to achieve higher pressures instead of testing with low pressures of 1 -2 bars. The spray flux acted as a covariate for several other experiments where it varied due to either wind, spray duration, or spray period. It could be interesting to analyse the data of these experiments through statistical means to investigate if any conclusion on the role of spray flux can be made.
- Spray duration: Longer spray durations tended to give lower icing rates in the initial stages. However, as time progressed, longer sprays resulted into higher icing rates as the effect of the substrate reduced after the formation of initial ice layers. Spray flux was a significant covariate, and the presented graphs are as result of a combination of spray duration and flux. Longer spray durations resulted in more ice stalactites.
- Spray period: Lower spray periods (more frequent sprays) gave lower icing rates in the initial stages but showed an increase as the icing progressed as the effect of the substrate reduced after the formation of initial ice layers. The spray flux, also here, was a significant covariate and should be considered while reading the results. Shorter spray periods or more frequent sprays give more ice stalactites.
- Salinity: Considering the first two readings in the experiment for salinity, the icing rates for seawater were lower than that of freshwater. The difference, however, was marginally more than the relative standard error in repetitions (experiment 0), suggesting that the salinity plays only a marginal role in the icing rates. In the third reading however, significant temperature deviations from the set temperatures were observed.

8.3. Future work with the experimental data

The current study gives a general idea of the trends for icing rates due to 8 different variables. The study also touches the topic of good practices for sea spray icing experiments by sharing the noteworthy experiences from the whole exercise. The real temperatures during the course of individual tests showed deviation from the set temperatures. The mean observed temperatures during individual experiments, too, varied when ideally, they should have remained constant. Reporting icing rates with these temperatures could include significant errors. The spray flux proved to be a significant covariate in many experiments. Inclusion of multiple variables that are highly interdependent calls for advanced statistical methods to make a correlation analysis and pinpoint how individual variables affect the icing rate. The huge amount of data collected from the 20 test that are presented in this article, calls for in investigation into the use of machine learning techniques for analysis. Moreover, variables such as spray flux, spray period, and spray duration, are a function of ship and wave characteristics. For the practical use of these variables, results have to be interpreted in terms of metocean conditions and ship characteristics. Lastly, the results have to be compared with existing models to ensure that the experimental data is suitable to be used as a basis for the development of a prediction model.

9. Acknowledgements

- The authors would like to thank all colleagues, friends, and family members that extended help during the construction and for taking measurements during this labour-intensive exercise.
- VikingNorsafe for glassfibre plate

10.References

[1] E. M. Samuelsen and R. G. Graversen, “Weather situation during observed ship-icing events off the coast of Northern Norway and the Svalbard archipelago,” *Weather Clim. Extrem.*, vol. 24, no. 9293, p. 100200, Jun. 2019, doi: 10.1016/j.wace.2019.100200.

[2] A. Kulyakhtin, “Numerical Modelling and Experiments on Sea Spray Icing,” Doctoral thesis. Department of Civil and Transport Engineering. Norwegian University of Science and Technology (NTNU), Norway, 2014.

[3] S. Deshpande, A. Sæterdal, and P.-A. Sundsbø, “Sea Spray Icing: The Physical Process and Review of Prediction Models and Winterization Techniques,” *J. Offshore Mech. Arct. Eng.*, vol. 143, no. 6, pp. 1–12, Dec. 2021, doi: 10.1115/1.4050892.

[4] A. Kulyakhtin and A. Tsarau, “A time-dependent model of marine icing with application of computational fluid dynamics,” *Cold Reg. Sci. Technol.*, vol. 104–105, pp. 33–44, Aug. 2014, doi: 10.1016/j.coldregions.2014.05.001.

[5] I. Horjen, “Numerical modeling of two-dimensional sea spray icing on vessel-mounted cylinders,” *Cold Reg. Sci. Technol.*, vol. 93, pp. 20–35, Sep. 2013, doi: 10.1016/j.coldregions.2013.05.003.

[6] T. W. Forest, E. P. Lozowski, and R. Gagnon, “Estimating marine icing on offshore structures using RIGICE04,” in *Proceedings of the International Workshop on Atmospheric Icing on Structures*

(IWAIS), Montreal, Canada., 2005, no. June.

[7] E. M. Samuelsen, K. Edvardsen, and R. G. Graversen, "Modelled and observed sea-spray icing in Arctic-Norwegian waters," *Cold Reg. Sci. Technol.*, vol. 134, pp. 54–81, Feb. 2017, doi: 10.1016/j.coldregions.2016.11.002.

[8] J. E. Overland, "Prediction of Vessel Icing for Near-Freezing Sea Temperatures," *Weather Forecast.*, vol. 5, no. 1, pp. 62–77, Mar. 1990, doi: 10.1175/1520-0434(1990)005<0062:POVIFN>2.0.CO;2.

[9] Stallabrass, "Trawler Icing - a Compilation of Work Done At N. R. C.," *Mech. Eng. Rep. MD-56, N.R.C. No. 19372 (National Res. Counc. Ottawa Canada)*, 1980.

[10] J. E. Overland, C. H. Pease, R. W. Preisendorfer, and A. L. Comiskey, "Prediction of Vessel Icing," *J. Clim. Appl. Meteorol.*, vol. 25, no. 12, pp. 1793–1806, Dec. 1986, doi: 10.1175/1520-0450(1986)025<1793:POVI>2.0.CO;2.

[11] C. C. Ryerson, "Superstructure spray and ice accretion on a large U.S. Coast Guard cutter," *Atmos. Res.*, vol. 36, no. 3–4, pp. 321–337, May 1995, doi: 10.1016/0169-8095(94)00045-F.

[12] J. Stallabrass and P. Hearty, "The Icing of cylinders in conditions of simulated freezing sea spray," 1967.

[13] A. Dehghani-Sanij, M. Mahmoodi, S. R. Dehghani, Y. S. Muzychka, and G. F. Naterer, "Experimental investigation of vertical marine surface icing in periodic spray and cold conditions," *J. Offshore Mech. Arct. Eng.*, vol. 141, no. 2, pp. 1–40, 2019, doi: 10.1115/1.4041394.

[14] A. Kulyakhtin and T. Engineering, "Sea spray icing : in-cloud evaporation . Semi- analytical and numerical investigations .," vol. 42, 2011.

[15] A. Kulyakhtin, O. Shipilova, B. Libby, and S. Løset, "Full-scale 3D CFD Simulation of Spray Impingement on a Vessel Produced by Ship-wave Interaction," *Proc. 21st IAHR Intl. Symp. Ice*, pp. 1129–1141, 2012.

[16] A. Hyldgård, D. Mortensen, K. Birkelund, O. Hansen, and E. V. Thomsen, "Autonomous multi-sensor micro-system for measurement of ocean water salinity," *Sensors Actuators A Phys.*, vol. 147, no. 2, pp. 474–484, Oct. 2008, doi: 10.1016/J.SNA.2008.06.004.

[17] A. Dehghani-sanij, Y. S. Muzychka, and G. F. Naterer, "Analysis of Ice Accretion on Vertical Surfaces of Marine Vessels and Structures in Arctic Conditions," in *Volume 7: Ocean Engineering*, May 2015, pp. 1–7, doi: 10.1115/OMAE2015-41306.

[18] K. F. Jones and E. L. Andreas, "Sea spray concentrations and the icing of fixed offshore structures," *Q. J. R. Meteorol. Soc.*, vol. 138, no. 662, pp. 131–144, Jan. 2012, doi: 10.1002/qj.897.

[19] S. Brohez, C. Delvosalle, and G. Marlair, "A two-thermocouples probe for radiation corrections of measured temperatures in compartment fires," *Fire Saf. J.*, vol. 39, no. 5, pp. 399–411, Jul. 2004, doi: 10.1016/J.FIRESAF.2004.03.002.

[20] CSGNetwork, "Water Density Calculator," 2011. http://www.csgnetwork.com/h2odenscalc.html (accessed Sep. 14, 2022).

[21] Matlab_Documentation, "Filtering and Smoothing Data - MATLAB & Simulink - MathWorks Nordic." https://se.mathworks.com/help/curvefit/smoothing-data.html (accessed Aug. 16, 2022).

[22] R. D. Brown and T. Agnew, “Characteristics of marine icing in Canadian waters.,” in *Proceedings of the International Workshop on Offshore Winds and Icing*, 1985, pp. 78–94.

[23] X. Chang *et al.*, “Research on ultrasonic-based investigation of mechanical properties of ice,” *Acta Oceanol. Sin.*, vol. 40, no. 10, pp. 97–105, 2021, doi: 10.1007/s13131-021-1890-3.

[24] *ISO 19906:*, 2nd ed. Petroleum and natural gas industries – Arctic offshore structures, 2019.

[25] M. C. Ortiz, L. A. Sarabia, M. S. Sánchez, and A. Herrero, “Quality of Analytical Measurements: Statistical Methods for Internal Validation,” in *Comprehensive Chemometrics*, vol. 1, Elsevier, 2009, pp. 17–76.

[26] S. Ferraris and L. M. Volpone, “ALUMINIUM ALLOYS IN THIRD MILLENNIUM SHIPBUILDING: MATERIALS, TECHNOLOGIES, PERSPECTIVES.,” *Fifth Int. Forum Alum. Ships.*, Oct. 2005.

[27] S. SUZUKI, R. MURAOKA, T. OBINATA, S. ENDO, T. HORITA, and K. OMATA, “Steel Products for Shipbuilding,” *JFE Tech. REPORT, 241*, Mar. 2004.

[28] VikingNorsafe, “VIKING Norsafe Life-Saving Equipment Norway AS MATHILDA-74,” VIKING Doc. No.: TSB-0045, Rev. No. 3, Mar. 2021. Accessed: Aug. 15, 2022. [Online]. Available: https://myviking.viking-life.com/en/Boats-and-davits/Boats/Conventional-lifeboats/p/P0301001030.

[29] RolledMetalProducts, “Aluminum 5052 data sheet.” 2017, [Online]. Available: rolledmetalproducts.com/wp-content/uploads/docs/Aluminum5052.pdf.

[30] A. A. Bhatti, Z. Barsoum, H. Murakawa, and I. Barsoum, “Influence of thermo-mechanical material properties of different steel grades on welding residual stresses and angular distortion,” *Mater. Des.*, vol. 65, pp. 878–889, Jan. 2015, doi: 10.1016/j.matdes.2014.10.019.

[31] G. B Vaggar, S. C Kamate, and P. V Badyankal, “Thermal Properties Characterization of Glass Fiber Hybrid Polymer Composite Materials,” *Int. J. Eng. Technol.*, vol. 7, no. 3.34, p. 455, Sep. 2018, doi: 10.14419/ijet.v7i3.34.19359.

[32] S. Wang and J. Qiu, “Enhancing thermal conductivity of glass fiber/polymer composites through carbon nanotubes incorporation,” *Compos. Part B Eng.*, vol. 41, no. 7, pp. 533–536, Oct. 2010, doi: 10.1016/j.compositesb.2010.07.002.

[33] L. Li, Y. Liu, Z. Zhang, and H. Hu, “Effects of thermal conductivity of airframe substrate on the dynamic ice accretion process pertinent to UAS inflight icing phenomena,” *Int. J. Heat Mass Transf.*, vol. 131, pp. 1184–1195, Mar. 2019, doi: 10.1016/J.IJHEATMASSTRANSFER.2018.11.132.

[34] E. P. Lozowski, K. Szilder, and L. Makkonen, “Computer simulation of marine ice accretion,” *Philos. Trans. R. Soc. London. Ser. A Math. Phys. Eng. Sci.*, vol. 358, no. 1776, pp. 2811–2845, Nov. 2000, doi: 10.1098/rsta.2000.0687.

[35] P. Dawson and S. L. Dawson, “Sharing successes and hiding failures: ‘reporting bias’ in learning and teaching research,” *https://doi.org/10.1080/03075079.2016.1258052*, vol. 43, no. 8, pp. 1405–1416, Aug. 2016, doi: 10.1080/03075079.2016.1258052.

[36] I. Horjen and S. Vefsnmo, “Mobile platform stability (MOPS) subproject 02 - icing (MOPS Report No. 15).,” 1984.

[37] R. D. Brown and P. Roebber, “The Scope of the ice accfretion problem in Canadian waters related

to offshore energy and transportation.," Canadian Climate Centre Report 85-13, 1985.

[38] W. P. Zakrzewski, "Icing of Fishing Vessels. Part I: Splashing a Ship With Spray.," 1986.